Check for updates

Plant Biotechnology Journal

WILEY

RESEARCH ARTICLE OPEN ACCESS

Engineering Cyanobacteria for High-Yield Photosynthetic Isoprene Production With Long-Term Phenotypic Stability

Kim N. Janssen[1] | Paul Bolay[1] | Adrian Tüllinghoff[2] | Jörg Toepel[2] | Daniel Spindler[2] | Bruno Bühler[2] | Pia Lindberg[1]

[1]Department of Chemistry—Ångström, Uppsala University, Uppsala, Sweden | [2]Department of Microbial Biotechnology, Helmholtz Centre for Environmental Research GmbH—UFZ, Leipzig, Germany

Correspondence: Pia Lindberg (pia.lindberg@kemi.uu.se)

Received: 27 June 2025 | **Revised:** 29 August 2025 | **Accepted:** 21 September 2025

Funding: This work was supported by the Swedish Energy Agency (38334-3), by the Carl Trygger Foundation for Scientific Research (18-224), and by the Horizon Europe project ALFAFUELS (GA 101122224). We acknowledge the use of the facilities of the Centre for Biocatalysis (MiKat) at the Helmholtz Centre for Environmental Research, which is supported by the European Regional Development Funds (EFRE, Europe funds Saxony, project no. 100361842) and the Helmholtz Association.

Keywords: cyanobacteria | isoprene | metabolic engineering | photobiotechnology | terpenoids

ABSTRACT

In light of the looming climate crisis, a key cornerstone for a sustainable bioeconomy is photosynthetic production of chemicals and fuels from CO_2 and water, powered by sunlight. Isoprene is a five-carbon volatile hydrocarbon with industrial use as a feedstock for rubber production and chemical synthesis and is, at present, generated from crude oil sources. It is, however, possible to produce isoprene using photoautotrophic microorganisms such as cyanobacteria, heterologously expressing the plant enzyme isoprene synthase. Here, we have employed diverse metabolic engineering strategies to develop new strains of the unicellular cyanobacterium *Synechocystis* sp. PCC 6803 capable of high-level isoprene production from CO_2, and have characterised the resulting strains regarding growth, stability and productivity. The new isoprene-producing strains address several challenges in large-scale photobiotechnological production such as genetic and metabolic stability, biosafety and thermotolerance. Moreover, we tested photosynthetic terpenoid production in photobioreactors under process-relevant conditions, achieving the highest volumetric productivities reported so far for a terpene or terpenoid product in cyanobacteria, reaching 148 mg L^{-1} day^{-1}. Furthermore, we identified and discussed process limitations, laying the foundation for further strain and process engineering towards highly efficient and stable cyanobacterial hydrocarbon production at large scale without selection pressure.

1 | Introduction

Cyanobacteria are a remarkable clade, being the inventors of oxygenic photosynthesis and playing crucial ecological roles for a large part of the history of life on earth (Demoulin et al. 2019). Moreover, cyanobacteria have gained interest as promising chassis for sustainable biotechnological applications like de novo synthesis of biofuels and commodity chemicals directly from CO_2 driven by sunlight via photosynthesis (Bolay et al. 2024), thereby avoiding use of fossil resources and agricultural feedstock. Cyanobacterial production performance remains a major issue, being mostly orders of magnitude below those of well-established heterotrophic hosts that achieve commercial competitiveness. Low product titres and space–time yields achieved with phototrophs, typically related to insufficient flux of fixed carbon towards the compound of interest, constitute key limitations for CO_2-based production with cyanobacteria (Nielsen et al. 2016), which increase production costs and prevent widespread commercial application. Thus, engineering the allocation of carbon towards precursor synthesis by increasing

Kim N. Janssen and Paul Bolay contributed equally to this article.

This is an open access article under the terms of the Creative Commons Attribution-NonCommercial-NoDerivs License, which permits use and distribution in any medium, provided the original work is properly cited, the use is non-commercial and no modifications or adaptations are made.

© 2025 The Author(s). *Plant Biotechnology Journal* published by Society for Experimental Biology and The Association of Applied Biologists and John Wiley & Sons Ltd.

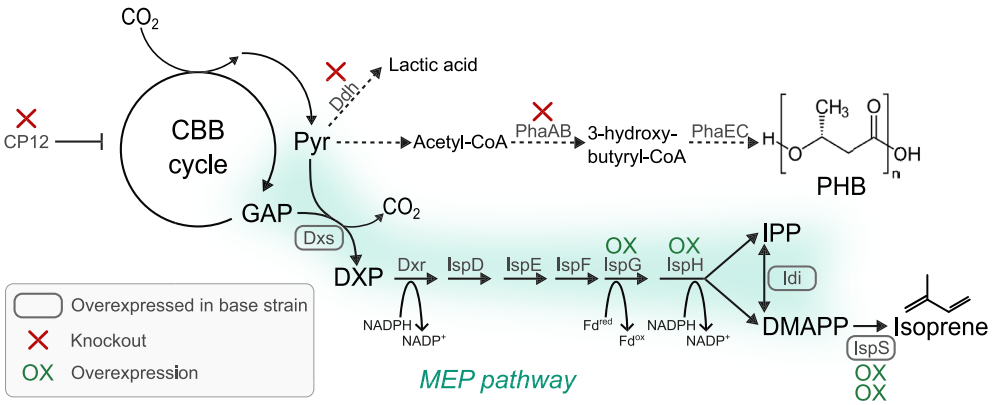

FIGURE 1 | Genetic and metabolic engineering of the base strains 1-IspS and KJ05. Central carbon metabolism, the MEP pathway and potentially competing biosynthesis pathways for PHB and lactic acid are shown. Genes encoding enzymes that are overexpressed in the base strains 1-IspS and KJ05 are indicated with a box. Further engineering is indicated with an X for gene knockouts and OX for overexpression of the respective gene. The MEP pathway is marked with a green background. CBB cycle, Calvin-Benson-Bassham cycle; DMAPP, dimethylallyl diphosphate; DXP, 1-deoxy-D-xylulose-5-phosphate; Dxr, DXP reductoisomerase; Dxs, DXP synthase; $Fd^{red/ox}$, ferredoxin reduced/oxidised; GAP, glyceraldehyde 3-phosphate; Idi, IPP isomerase; IPP, isopentenyl diphosphate; IspD, MEP cytidylyltransferase, IspE, CDP-ME kinase; IspF, ME-CDP synthase; IspG, HMBDP synthase; IspH, HMBDP reductase; IspS, isoprene synthase; NADP(H), nicotinamide adenine dinucleotide phosphate; Pyr, pyruvate.

the flux through anabolic pathways of interest is a promising strategy to get closer to the commercialisation of cyanobacterial processes.

Cyanobacterial production strains for large-scale outdoor cultivation, which is required to reduce costs and energy consumption, need to fulfill biosafety criteria, that is, absence of biohazardous elements like antibiotic resistance genes and broad-range elements, for example, plasmids that can swiftly be horizontally transferred among different species (Čelešnik et al. 2016). Moreover, a major risk for large-scale bioprocesses typically including growth over many generations is the evolvement of population heterogeneity involving low- or non-producing variants with the tendency to overgrow productive individuals and hamper overall productivity (Rugbjerg and Olsson 2020). Genetic instability is widely observed for cyanobacteria (Menin et al. 2019; Mustila et al. 2021; Yunus and Jones 2018), yet rarely reported in genetic engineering studies that typically rely on the presence of antibiotics in growth media (Jones 2014). Taken together, the generation and application of markerless production strains with stable phenotypes is of both economic and ecological interest. Modern genome editing techniques, such as CRISPR gene editing (Behler et al. 2018), allow genetic engineering without antibiotic resistance cassette knock-ins. The genetic stability and, as a result, phenotypic stability of such marker-less production strains has, however, not been demonstrated. One compound currently generated from crude oil, which can be sustainably produced from CO_2 and sunlight by cyanobacteria, is isoprene. This hemiterpene is largely used for rubber production but has a plethora of other industrial applications and could serve as a raw material for the sustainable production of chemicals and jet fuel (Cid Gomes et al. 2025; Rana et al. 2022). While isoprene is naturally produced by a variety of plants, its formation in cyanobacteria requires the heterologous introduction of a plant-derived isoprene synthase (IspS) (Lindberg et al. 2010). Its substrate dimethylallyl pyrophosphate (DMAPP) is generated via the 2-*C*-methyl-D-erythritol 4-phosphate (MEP) pathway (Figure 1), which is fed by the photosynthetic products pyruvate (Pyr) and glyceraldehyde 3-phosphate (G3P; Lichtenthaler 1999; Rohmer et al. 1996). Due to its volatility and low boiling point, isoprene is constantly released from the culture, allowing for continuous production and simple assessment of production performance.

Since the pioneering work that established isoprene production in cyanobacteria 15 years ago (Lindberg et al. 2010), substantial progress has been made in identifying enzymes which, when overexpressed, have beneficial effects on the production. Moreover, the understanding of the tight, multi-layered metabolic regulation of the MEP pathway, its inherent bottlenecks and how to circumvent them has been ever-growing (for reviews, see Chaves and Melis 2018; Rodrigues and Lindberg 2021a). While catalytically superior isoprene synthases have been identified and successfully transferred to cyanobacteria, overexpression of genes encoding selected heterologous and native MEP pathway enzymes has been proven beneficial to relieve bottlenecks and further increase isoprene productivity (Englund et al. 2018; Gao et al. 2016).

1-Deoxy-D-xylulose-5-phosphate (DXP) synthesis from Pyr and G3P catalysed by DXP synthase (Dxs) constitutes a critical step in the MEP pathway (Figure 1). In *Escherichia coli*, flux control analysis has identified Dxs as the rate-limiting enzyme in the MEP pathway (Volke et al. 2019), with intracellular concentrations of its substrates considerably below respective Michaelis–Menten constants (Volke et al. 2019). This is illustrated by the fact that increasing G3P and Pyr concentrations results in a similar increase in MEP pathway flux (Liu et al. 2013). Thus, engineering upstream carbon metabolism is expected to enhance isoprene productivity. Apart from thermodynamic considerations, a growing body of work suggests feedback inhibition of the Dxs homodimer by dimethylallyl pyrophosphate and isopentenyl pyrophosphate (IPP), with the actual mechanism being a subject of debate (Banerjee et al. 2013; Di et al. 2023). Additionally, IspS was also shown to be inhibited by IPP (Gao et al. 2016). These findings clearly illustrate that DMAPP/IPP concentration and ratio are key targets for increasing the MEP flux and eventually isoprene biosynthesis.

14677652, 2026, 3, Downloaded from https://onlinelibrary.wiley.com/doi/10.1111/pbi.70395 by Uppsala University, Wiley Online Library on [27/05/2026]. See the Terms and Conditions (https://onlinelibrary.wiley.com/terms-and-conditions) on Wiley Online Library for rules of use; OA articles are governed by the applicable Creative Commons License

The highest reported volumetric isoprene productivity by a cyanobacterium was achieved with a *Synechococcus elongatus* strain overexpressing an *ispS* gene from *Eucalyptus globulus*, which was translationally fused to the isopentenyl-diphosphate delta-isomerase gene *idi* from *S. cerevisiae*. Moreover, native *ispG* encoding the MEP pathway enzyme 2-C-methyl-D-erythritol-2,4-cyclodiphosphate reductase was constitutively overexpressed, as IspG was identified as a bottleneck (Gao et al. 2016). This enabled cumulative production of 1.26 g L^{-1} isoprene in 21 days of cultivation in 20 mL small-scale bioreactors. As a comparison, heterotrophic isoprene production from glucose with engineered *E. coli* strains has been shown to yield up to 60 g L^{-1} in 60 h of fed-batch fermentation with a maximal volumetric productivity of 2 g L^{-1} h^{-1} (Whited et al. 2010).

In this study, we set out to engineer the unicellular cyanobacterium *Synechocystis* sp. PCC 6803 (hereafter *Synechocystis*) for enhanced and long-term stable production of isoprene in the absence of antibiotic selection pressure. Further, the performances of selected strains were evaluated in lab-scale bioreactors.

2 | Results and Discussion

2.1 | Isoprene-Producing *Synechocystis* Strains Are Highly Stable Without Selection Pressure

Given the aforementioned considerations regarding biosafety as well as genetic stability, we set out to generate a markerless *Synechocystis* strain for the production of isoprene. For this, we utilised the previously published strain "IspS" (Rana et al. 2022; here called 1-IspS), which overexpresses the genes encoding Dxs from *Plectranthus barbatus* (also termed *Coleus forskohlii*; Englund et al. 2015) and Idi from *Synechocystis* in one operon and IspS from *E. globulus* (hereafter referred to as IspS; Figures 1 and 2A) in a second operon, both under control of P*trc* promoters (Camsund et al. 2014; Rodrigues et al. 2023). This strain was originally generated by the introduction of the heterologous gene cassette into "Neutral Site I" (*slr0168*) via homologous recombination and subsequent selection on kanamycin to ensure full segregation (Figure 2A, Table S1). Removal of the kanamycin resistance gene in this strain has two benefits: it enhances biosafety for this specific strain and allows further engineering, such as the introduction of additional genetic elements with selection on kanamycin. For large-scale applications, a genetically and metabolically stable strain without the need for the addition of antibiotics also reduces cultivation costs. To delete the kanamycin resistance cassette, a replicative CRISPR plasmid carrying a gene encoding a Cas12 endonuclease also called Cpf1 (Ungerer and Pakrasi 2016), a gRNA sequence homologous to the kanamycin resistance gene and a homology repair cassette was temporarily introduced into the 1-IspS strain. Following successful genome editing, the CRISPR plasmid was cured to obtain the new markerless strain KJ05, which does not carry any antibiotic resistance genes (Figure 2A, Table S1).

Subsequently, KJ05 was compared to the original 1-IspS strain, both grown with and without kanamycin, to assess genetic and metabolic stability. The strains were inoculated in shake flasks, and growth as well as isoprene formation capability was monitored over time. It has been shown in a previous study that isoprene production in the 1-IspS strain increases thermotolerance of the cells and that a temperature increase to 40°C led to increased isoprene production rates (Rodrigues et al. 2023). Therefore, we regularly transferred culture samples to 40°C and high carbonate conditions in order to test their isoprene formation capability. Growth was slightly reduced in the presence of kanamycin (Figure 2B). After 3 days of cultivation at 30°C, the isoprene production performance of both 1-IspS and KJ05 grown without antibiotics was significantly higher compared to 1-IspS grown with kanamycin, suggesting that the presence of kanamycin compromised the isoprene formation capability (Figure 2C). After 11 days, fresh BG11 with or without kanamycin was supplemented to the cultures, and isoprene production was assessed again on day 14, followed by re-inoculation in fresh BG11 with or without kanamycin and isoprene production capability assessment after three days on day 17 (Figure 2C). Interestingly, cells from all cultures produced isoprene at higher rates after 14 and 17 days than after 3 days of cultivation (Figure 2C). In contrast to cells harvested at comparably low cell density (day 3, day 17), the negative impact of kanamycin on isoprene formation appeared to be mitigated after cultivation to higher cell density (day 14). Cultivation was continued for an overall 200 days, which involved re-inoculation every two to three weeks (Figure 2D,E). Isoprene production was monitored three days after each re-inoculation and thus with cells harvested in the same growth phase as those harvested after 3 and 17 days of cultivation (Figure 2B,C). After about 50 days, no clear negative impact of kanamycin on isoprene production was observed anymore, and cells of all three cultures maintained similar specific isoprene production activities, stabilising at ~50% of the maximal rates determined after 3–17 days.

Overall, the engineered strains showed convincing genetic and phenotypic stability that led to consistent isoprene production in the absence of selection pressure for more than 6 months. These results suggest that no pressure towards evasive mutations appears to be imposed, at least not under the cultivation conditions applied. Increased flux through the MEP pathway towards isoprene could even be beneficial for the cells, as isoprene has been shown to protect plants from oxidative stress, via inhibition of reactive oxygen species (ROS) accumulation and increased levels of antioxidants such as ascorbate (Vickers, Possell, et al. 2009). Moreover, isoprene synthases generally operate at a higher K_m for DMAPP than other DMAPP-consuming enzymes, e.g., monoterpene or sesquiterpene synthases (Schnitzler et al. 2005; Sharkey and Aspland 2013; Ye et al. 2016). Isoprene production at rates observed in this study thus is not expected to compete with essential physiological functions based on other MEP pathway-derived metabolites. Assuming growth for the serial dilutions similar to the one shown in Figure 2B, the long-term experiment (Figure 2D) corresponds to more than 70 generations that maintained heterologous gene expression and isoprene formation proficiency in the absence of any selection pressure. To our knowledge, this is by far the longest stable production capacity by a genetically engineered cyanobacterium ever demonstrated and lays the foundation for isoprene

14677652, 2026, 3, Downloaded from https://onlinelibrary.wiley.com/doi/10.1111/pbi.70395 by Uppsala University, Wiley Online Library on [27/05/2026]. See the Terms and Conditions (https://onlinelibrary.wiley.com/terms-and-conditions) on Wiley Online Library for rules of use; OA articles are governed by the applicable Creative Commons License

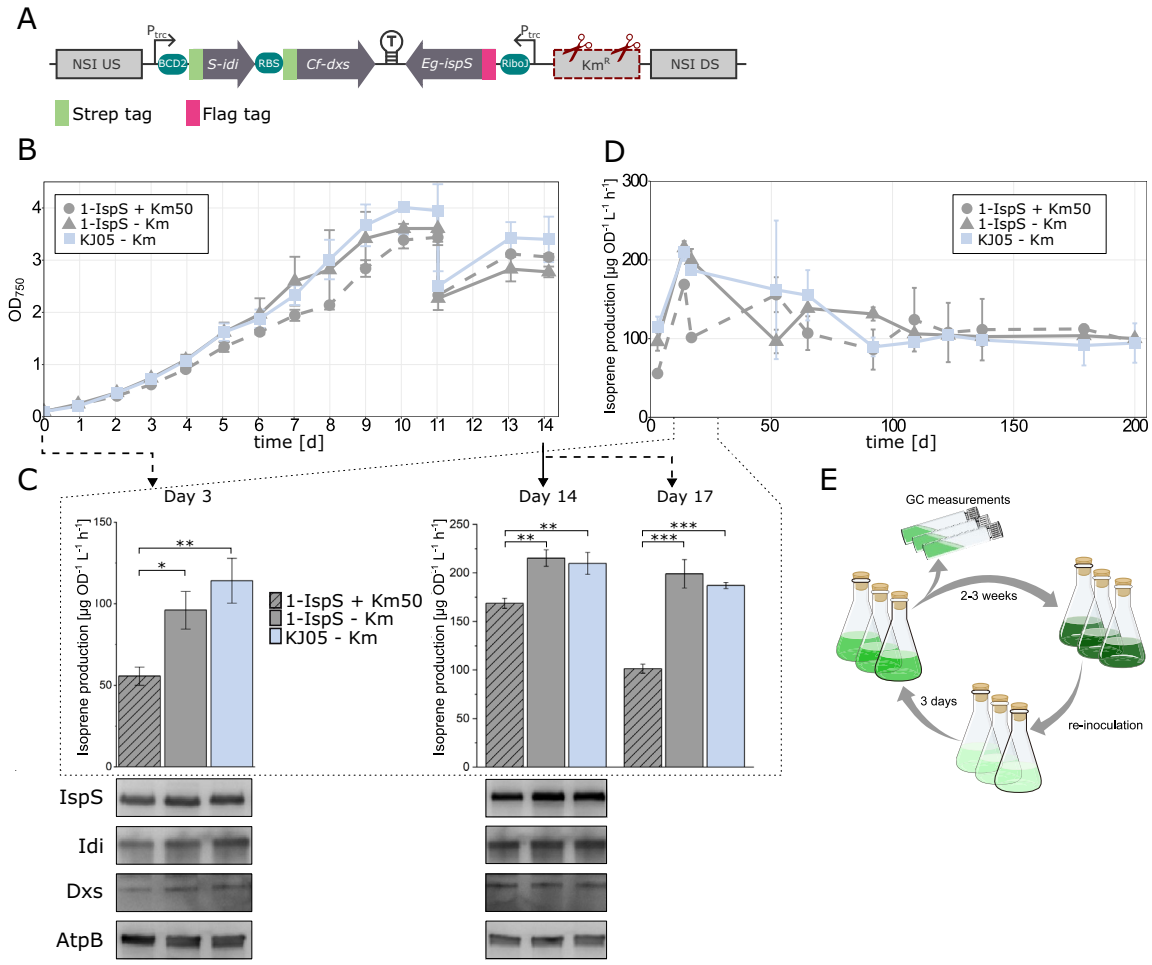

FIGURE 2 | Removal of antibiotic resistance cassette and long-term production proving strain stability. (A) Schematic representation of gene cassette enabling isoprene production, integrated into neutral site 1 (NSI; *slr0168*); red scissors indicate removal of antibiotic resistance gene. (B) Growth curves of the first 14 days in 25 mL batch cultures, grown at 30°C in TES buffered BG11 medium with (dashed line, + Km50) or without (solid lines, − Km) 50 µg mL^{-1} kanamycin at 50 µmol photons m^{-2} s^{-1} and ambient CO_2. Ten mL of fresh medium were replenished on day 11. (C) Isoprene production rates determined during incubation at 40°C at 120 µmol photons m^{-2} s^{-1} of culture samples transferred into closed vials in 20 mL total medium volume and supplemented with 50 mM sodium bicarbonate. Cultures for day three measurements were grown in parallel, inoculated from the same pre-cultures; cultures displayed on day 14 were directly sampled from batch cultures displaced in (B); cultures displayed on day 17 were re-inoculated from batch culture at OD_{750} of 0.1 on day 14. Grey colour indicates the base strain 1-IspS, blue colour the edited strain KJ05 without kanamycin resistance. Bottom panel: Western blot of proteins encoded by heterologously overexpressed genes after three, 14 and 17 days of cultivation. AtpB was used as a loading control. Statistical significance was tested via Tukey's HSD test: *$p < 0.05$, **$p < 0.01$, ***$p < 0.001$. (D) Isoprene production rates of cells cultivated over 200 days with periodic re-inoculation to a starting OD_{750} of 0.1 in fresh medium (after 14 days for the first time) following the scheme shown in panel E. Isoprene production was determined three days after re-inoculation (e.g., on day 17). Error bars represent standard deviations of three biological triplicates. AtpB, ATP synthase β-subunit; *Cf-dxs*, 1-deoxy-D-xylulose-5-phosphate synthase gene from *Coleus forskohlii*; d, days; DS, downstream; *Eg-ispS*, isoprene synthase gene from *Eucalyptus globulus*; GC, gas chromatography; Km^R, kanamycin resistance cassette; NSI, neutral site 1; *S-idi*, isopentenyl-diphosphate delta-isomerase gene from *Synechocystis*; US, upstream.

as an ideal target chemical to be produced by cyanobacteria. The KJ05 strain thus augurs well to meet the requirements for large-scale, long-term outdoor cultivation, which necessitates a high number of generations that maintain phenotypic stability to achieve profitable titres (Borowitzka and Vonshak 2017). Moreover, biohazardous genes, whose proliferation in nature must be avoided, are absent in the KJ05 strain. Given the apparent under-reporting of cyanobacterial strain stability or lack thereof (Jones 2014), we hope to set an example for the characterisation of cyanobacterial production strains under relevant long time scales and in absence of antibiotics and biohazardous genes in order to address the present challenges in upscaling of photosynthetic chemical production.

2.2 | Identification and Relief of Isoprene Synthase as Key Limitation

Given the stable and reliable isoprene formation capacity of the KJ05 strain, we chose to use this strain as a platform for further genetic engineering approaches to increase isoprene productivity by overproducing a selection of enzymes whose activity could represent a bottleneck towards isoprene formation. Simultaneously, we aimed to knock out competing pathways or metabolic regulators that might limit the flux of carbon towards isoprene. Simultaneous deletion and insertion were targeted by choosing *phaAB*, *cp12* and *ddh* as insertion sites for the overexpression of anticipated bottleneck

14677652, 2026, 3, Downloaded from https://onlinelibrary.wiley.com/doi/10.1111/pbi.70395 by Uppsala University, Wiley Online Library on [27/05/2026]. See the Terms and Conditions (https://onlinelibrary.wiley.com/terms-and-conditions) on Wiley Online Library for rules of use; OA articles are governed by the applicable Creative Commons License

genes. The *phaAB* genes are required for polyhydroxybutyrate (PHB) production (Figure 1), an energy and carbon storage compound in cyanobacteria. PHB is synthesised in an NADPH-consuming, multi-step process from acetyl-CoA. It has been shown that PHB synthesis is dispensable for cellular viability under all conditions tested so far, while its physiological role remains a subject of debate (Koch et al. 2020). The *cp12* gene encodes a small protein that regulates carbon flux through the Calvin-Benson-Bassham (CBB) cycle via direct interaction with and thus inhibition of glyceraldehyde 3-phosphate dehydrogenase (GapDH) and phosphoribulokinase (PRK) (Wedel and Soll 1998) in response to changes in the redox state of the cell (Lucius et al. 2022; Miao et al. 2023; reviewed in Lucius and Hagemann 2024). Recent work in *Synechocystis* suggested that the CP12 protein plays a crucial role in redox regulation beyond its prominent role in the CBB cycle (Blanc-Garin et al. 2022). The authors of this study were able to double production of the two terpenes bisabolene and limonene by knocking out *cp12*, without affecting growth of *Synechocystis* (Blanc-Garin et al. 2022). Lastly, we knocked out the *ddh* gene, encoding D-lactate dehydrogenase (Ddh), converting pyruvate (Figure 1), one of the substrates of the MEP pathway, to lactate. We anticipated that knockout of *ddh* might allocate more carbon towards the MEP pathway by relieving carbon flux towards a competing pathway. To compare the potential of *phaAB*, *cp12* and *ddh* as insertion sites in the KJ05 background, we first generated knockout strains using chloramphenicol (CmR) or erythromycin (EmR) resistance cassettes, yielding the strains KJ18, KJ19 and KJ46, respectively (Figure 3A, Table S1). None of the knockouts led to an increase in isoprene production, but rather a slight decrease, with KJ19 (Δ*cp12*) showing the most pronounced reduction in isoprene formation of 33% (Figure 3B).

Based on these results, we selected *phaAB* as the insertion site for overexpression of potential bottleneck genes. As target genes, we chose the native *ispG* gene from *Synechocystis* (*S-ispG*), as IspG has been proven to be a bottleneck for isoprene synthesis in another cyanobacterial host (Gao et al. 2016), in combination with one of two different *ispH* genes encoding (*E*)-4-hydroxy-3-methylbut-2-enyl pyrophosphate reductases providing favourable DMAPP/IPP ratios derived from the two plants *Populus trichocarpa* (Pt-IspH) and *Ricinus communis* (Rc-IspH) (Bongers et al. 2020). While bacterial IspHs, such as the one of *E.coli*, generate a DMAPP/IPP ratio of less than 3, IspHs of *P. trichocarpa* and *R. communis* were shown to generate a DMAPP/IPP ratio of over 15 (Bongers et al. 2020). Consequently, deploying these IspHs may improve isoprene production due to a relief of enzyme inhibition combined with additional substrate provision for the terminal isoprene synthase. Lastly, we overexpressed the isoprene synthase gene *ispS* from *E. globulus* (*Eg-ispS*). Constructs for overexpression of *Rc-ispH* and *S-ispG*, *Pt-ispH* and *S-ispG* and *Eg-ispS* were introduced into the *phaAB* locus of the markerless background strain KJ05, resulting in the new strains KJ11 (*phaAB*: *Rc-ispH, S-ispG*), KJ16 (*phaAB: Pt-ispH, S-ispG*) and KJ26 (*phaAB: Eg-ispS*), respectively (Figure 3C, Table S1). After fully segregated strains were obtained (Figure S2), isoprene production was compared with that of KJ05, and Western blot analyses were performed to confirm successful expression of all heterologous genes (Figure 3C). The only strain that showed elevated isoprene formation was KJ26, expressing an additional *ispS* copy, leading to a roughly two-fold increase in isoprene formation. These results clearly illustrated that flux through IspS represents a central rate-limiting step.

In cyanobacteria, a superior performance of Eg-IspS over IspSs from other plant hosts has been reported (Englund et al. 2018; Gao et al. 2016) and attributed to its lower K_m (0.16 mM) and thus higher affinity for DMAPP compared to most other IspSs that have been studied (Sharkey and Aspland 2013; Schnitzler et al. 2005). To our knowledge, the intracellular concentration of DMAPP in *Synechocystis* has not been investigated, yet. However, in *S. elongatus* PCC7942 wild-type cells, Gao et al. measured a DMAPP concentration of 2.8 μM, which is far below the K_m reported for Eg-IspS. Upon overexpression of *Eg-ispS*, *Saccharomyces cerevisiae idi* and the native *dxs* (both also overexpressed in the (parent) strains used in this study), DMAPP concentrations increased slightly to 4.8 μM (Gao et al. 2016). If we expect similar orders of magnitude in our engineered *Synechocystis* strains, Eg-IspS would operate at a low reaction rate and could additionally be inhibited by intracellular IPP (Gao et al. 2016), therefore still representing a possible bottleneck for isoprene production. Upon increase of the IspS level in the KJ26 strain, this inhibitory effect may become reduced, as elevated DMAPP consumption should lead to a decrease in IPP concentration with Idi establishing a fixed DMAPP/IPP ratio. This, together with the overall higher IspS activity, then leads to increased isoprene production.

As previously mentioned, higher levels of MEP pathway substrates substantially increase pathway flux (Liu et al. 2013). Improving carbon flux towards desired pathways is even more crucial in photosynthetic hosts such as *Synechocystis*, relying on CO_2 uptake rates that are significantly lower than glucose uptake rates of heterotrophic strains (Zavřel et al. 2017).

As the IspS bottleneck seemed to be at least partly relieved by the expression of a second copy of the isoprene synthase gene, we speculated that tweaking carbon and redox metabolism via knockout of *cp12* or *ddh* might have a more pronounced effect, with IspS causing an increased MEP flux. This prompted us to test also the two genomic loci *ddh* and *cp12* for *Eg-ispS* expression, resulting in the strains KJ20 (*cp12: Eg-ispS*) and KJ21 (*ddh: Eg-ispS*). *Eg-ispS* overexpression from either of the tested loci increased isoprene production by about 2-fold (Figure 3D). However, the same pattern was observed as in the control knockouts (Figure 3B), with KJ26 (*phaAB: Eg-ispS*) showing the highest productivity and KJ20 (*cp12: Eg-ispS*) the lowest (Figure 3D). Thus, no additional positive effect on isoprene production was observed, suggesting that there might still be a bottleneck within the MEP pathway or that the selected targets are not effective under the conditions tested.

2.3 | Further Improvement and Physiological Analysis of Isoprene Producing Strains

As the introduction of a second copy of the *ispS* gene doubled isoprene production, we further tested the introduction of *Eg-ispS* genes into the *ddh* loci of strains KJ11 (*phaAB: Rc-ispH, S-ispG*) and KJ16 (*phaAB: Pt-ispH, S-ispG*) as a second copy and

14677652, 2026, 3, Downloaded from https://onlinelibrary.wiley.com/doi/10.1111/pbi.70395 by Uppsala University, Wiley Online Library on [27/05/2026]. See the Terms and Conditions (https://onlinelibrary.wiley.com/terms-and-conditions) on Wiley Online Library for rules of use; OA articles are governed by the applicable Creative Commons License

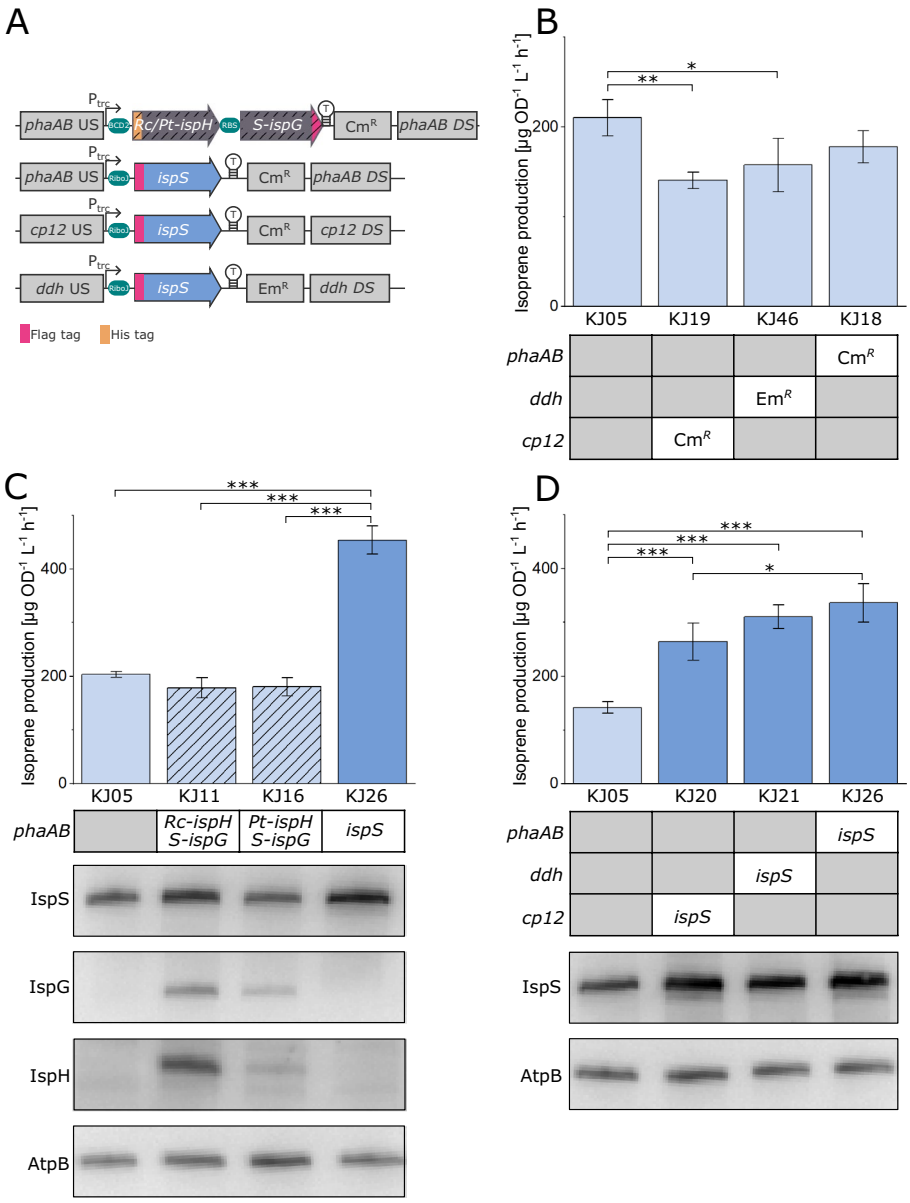

FIGURE 3 | Improvement of isoprene production via (simultaneous) deletion and insertion approaches. (A) Schematic representation of *ispS* or *ispGH* cassettes introduced into *phaAB*, *ddh*, or *cp12* sites. (BCD) Effects on isoprene production of *phaAB*, *ddh*, or *cp12* deletion (B) of *ispGH* or *Eg-ispS* overexpression from the *phaAB* site (C) and of *Eg-ispS* overexpression from different insertion sites (D), including Western blots for overexpressed proteins with AtpB as loading control. Different shades of blue indicate strains with one or two *ispS* copies inserted into the genome. Diagonal patterns indicate additional overexpression of *ispGH* genes. Error bars represent standard deviations of ≥3 biological replicates. Statistical significance was tested via Tukey's HSD test $*p<0.05$, $**p<0.01$, $***p<0.001$. Cm^R, chloramphenicol resistance cassette; *ddh*, D-lactate dehydrogenase gene; DS, downstream; Em^R, erythromycin resistance cassette; *phaAB*, acetyl-CoA acetyltransferase and acetoacetyl-CoA reductase genes, *Rc/Pt-ispH*, (E)-4-hydroxy-3-methylbut-2-enyl pyrophosphate reductase gene from *Ricinus communis/Populus trichocarpa*, *S-ispG*, 2-C-methyl-D-erythritol-2,4-cyclodiphosphate reductase gene from *SynechocystisI*; US, upstream.

of strains KJ26 (*phaAB: Eg-ispS*) and KJ20 (*cp12: Eg-ispS*) as a third copy (Table S1). This allowed us to assess whether (i) IspS still represents a bottleneck that would profit from a third gene copy, (ii) if overexpression of S-*ispG* and/or altered DMAPP/IPP ratios caused by the plant-derived IspHs could relieve potential new bottlenecks (Gao et al. 2016) in the presence of two *ispS* copies and (iii) whether dysregulated carbon and redox metabolism upon *cp12* knockout could increase MEP flux in the presence of three *ispS* gene copies. The only modification that yielded a further increase in productivity compared to strain KJ26 was another copy of *ispS* in this very strain, resulting in strain KJ27 (*phaAB Eg-ispS; ddh: Eg-ispS*; Figure 4A). This increase in comparison to strain KJ26, however, was only about 20%, showing that introducing a third copy had a less pronounced effect than the second copy that yielded >100% increase. A third copy in KJ29 (*cp12: Eg-ispS; ddh: Eg-ispS*) increased isoprene productivity over that of the parent strain KJ20 (*cp12: Eg-ispS*; Figure 4A) but did not reach the level of KJ27.

The reduced impact of the third copy compared to the second copy can be attributed to various factors. If the IspS bottleneck is already largely relieved by the second copy, more IspS

14677652, 2026, 3, Downloaded from https://onlinelibrary.wiley.com/doi/10.1111/pbi.70395 by Uppsala University, Wiley Online Library on [27/05/2026]. See the Terms and Conditions (https://onlinelibrary.wiley.com/terms-and-conditions) on Wiley Online Library for rules of use; OA articles are governed by the applicable Creative Commons License

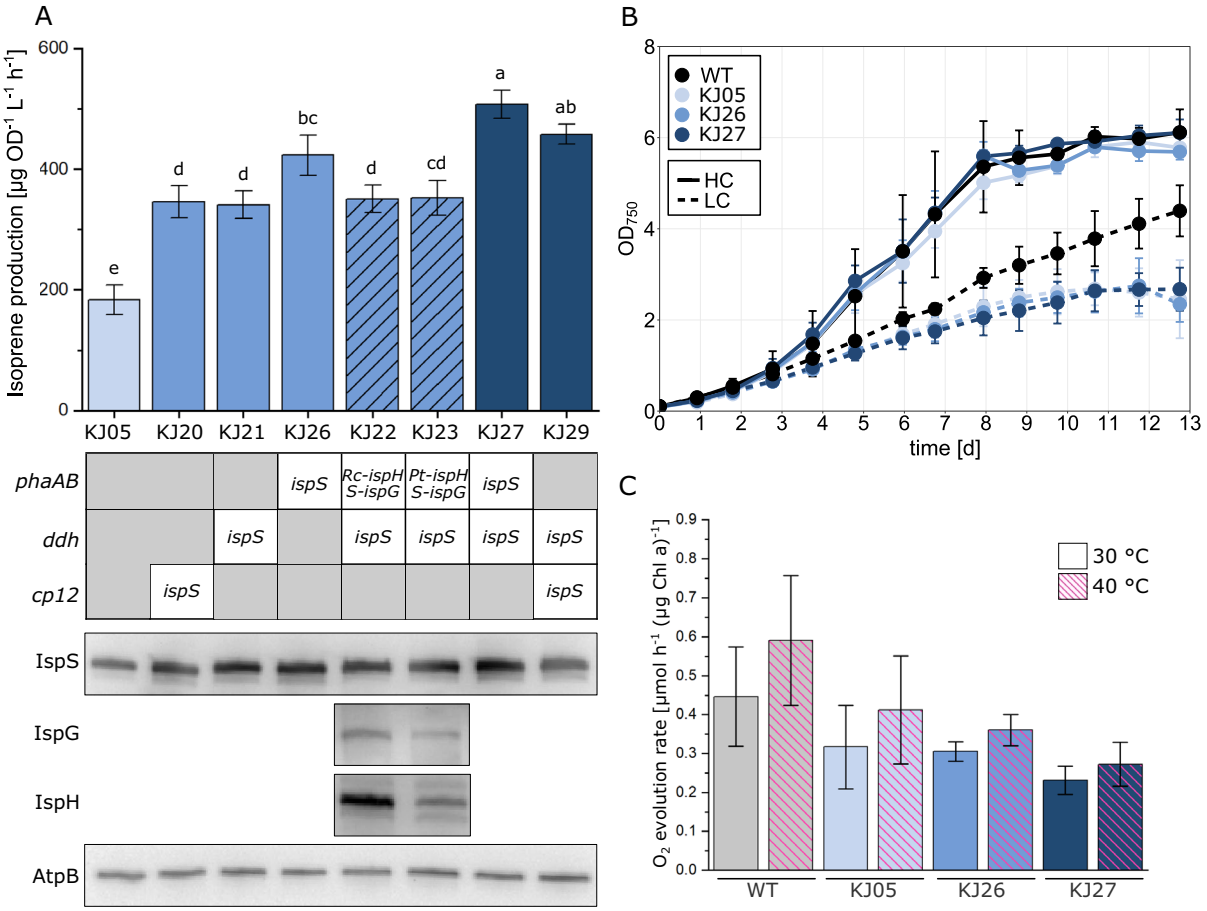

FIGURE 4 | Characterisation of isoprene-producing strains with increased *ispS* copy number. (A) Comparison of strains co-expressing a third *ispS* copy or *ispGH*. Top panel: Specific isoprene formation rates. Different shades of blue indicate strains with one, two, or three *ispS* copies inserted into the genome. Diagonal patterns indicates additional overexpression of *ispGH* genes. Statistical significance was tested via Tukey's HSD test; different letters indicate significant difference; identical letters indicate no significant difference with $p < 0.05$. Error bars represent standard deviations of three biological replicates. Bottom panel: Western blot analysis of overexpressed proteins. AtpB was used as a loading control. (B) Growth comparison of selected strains grown in 25 mL batch cultures in BG11 medium without addition of antibiotics at ambient CO_2 (LC; dashed line) and supplemented with 50 mM sodium bicarbonate every three days (HC; solid line). (C) Comparison of specific O_2 evolution rates of strains with increasing *ispS* copy number measured under saturating light conditions. O_2 evolution was measured at both 30°C (no pattern) and 40°C (magenta diagonal pattern) for cells of each strain cultivated at 30°C and 50 µmol photons $m^{-2}s^{-1}$. All error bars represent standard deviations of 3 biological replicates. AtpB, ATP synthase β-subunit; Chl a, chlorophyll a; d, days; *ddh*, D-lactate dehydrogenase gene; HC, high carbon; *ispS*, isoprene synthase gene from *Eucalyptus globulus*; LC, low carbon; *phaAB*, acetyl-CoA acetyltransferase and acetoacetyl-CoA reductase genes; *Rc/Pt-ispH*, (E)-4-hydroxy-3-methylbut-2-enyl pyrophosphate reductase gene from *Ricinus communis/Populus trichocarpa*; *S-ispG*, 2-C-methyl-D-erythritol-2,4-cyclodiphosphate reductase gene from *Synechocystis*.

protein abundance would not further impose an increased conversion of DMAPP to isoprene, as the substrate would be limiting. Therefore, another bottleneck within or upstream of the MEP pathway would have to be identified. Semi-quantitative Western blot analysis of the flag-tagged IspS band revealed that, in the strains with one and two *ispS* copies, the relative flag-IspS signal intensity corresponds to the isoprene production pattern (Figure S1), that is, the double-copy strains showed about twice the band intensity compared to KJ05. For the strains with a third genomic copy of *ispS*, however, we rather detected a decreased signal intensity compared to the two-copy strains, indicating that a third *ispS* copy did not lead to an increase in protein levels and that IspS still may constitute a limiting factor. This could be a result of the overexpression strategy. All *ispS* gene copies are expressed using the same promoter (P_{trc}), genetic insulator RiboJ and ribosomal binding site. Limitation could occur on any level of gene expression. On a transcriptional level, the recruitment of RNA polymerase and sigma factors for transcription from all promoters may become limiting (Bae et al. 2008). Translation could be limited when high amounts of IspS mRNAs with identical ribosomal binding sites compete for translation initiation with all cellular transcripts. Testing variations of different genetic elements thus could potentially enhance gene expression and lead to a further increase in IspS protein abundance and therefore isoprene production, given that DMAPP conversion to isoprene still represents a bottleneck.

To assess how isoprene production affects growth and photosynthetic activity of the cells, we compared strains exhibiting different productivity levels, i.e., KJ05, KJ26 (*phaAB: Eg-ispS*), and KJ27 (*phaAB: Eg-ispS; ddh: Eg-ispS*), and the wild

14677652, 2026, 3, Downloaded from https://onlinelibrary.wiley.com/doi/10.1111/pbi.70395 by Uppsala University, Wiley Online Library on [27/05/2026]. See the Terms and Conditions (https://onlinelibrary.wiley.com/terms-and-conditions) on Wiley Online Library for rules of use; OA articles are governed by the applicable Creative Commons License

type (WT) strain regarding growth and oxygen evolution. It was previously shown that isoprene production in *S. elongatus* PCC 7942 strains does not significantly affect carbon flux towards biomass (Gao et al. 2016). This involved increased photosynthetic activity leading to elevated O_2 evolution and upregulation of carbon fixation (Gao et al. 2016). For KJ05, KJ26 and KJ27, however, we observed reduced growth compared to the WT under standard conditions at 30°C and ambient CO_2. This especially became evident after six days of cultivation, when growth of isoprene-producing strains progressively slowed down, while WT cultures continued to grow linearly, reaching almost double the cell density after 13 days (Figure 4B, Table S3). However, isoprene-producing and WT strains grown under the same conditions but supplemented with 50 mM sodium bicarbonate every three days, did not show any differences, indicating that, without carbon supplementation, carbon availability limited growth of isoprene-producing strains (Figure 4B, Table S3). With isoprene as an additional carbon sink, cells require more carbon to reach the same cell density as the WT. Thus, carbon fixation obviously is increased in isoprene-producing strains, leading to a more pronounced carbon limitation when grown under low-carbon conditions.

The unaffected carbon flux towards biomass in isoprene-producing strains during linear growth with sufficient carbon available prompted us to further assess the impact of isoprene production on photosynthetic activity via the quantification of O_2 evolution. This was done at both of the two temperatures used so far for cultivation and production, 30°C and 40°C, respectively. In contrast to the previously observed increase in O_2 evolution rates of isoprene-producing *S. elongatus* PCC 7942 strains (Gao et al. 2016), strains tested in this study exhibited a decrease in O_2 evolution with increasing isoprene production capacity at both temperatures (Figure 4C). However, O_2 evolution itself does not represent the overall photosynthetic activity but only photosystem II (PSII)-driven water oxidation. Released electrons can follow linear electron flow (LEF), where they are transferred directly to ferredoxin and $NADP^+$, or be recycled via cyclic electron flow (CEF) around photosystem I (PSI), resulting in additional ATP production. The ATP/NADPH ratio required for biomass production and maintenance is ≥ 2 (Knoop and Steuer 2015; Shabestary and Hudson 2016), whereas a lower ratio is required for redox-intensive pathways such as terpene synthesis (Shabestary and Hudson 2016). The observed decrease in O_2 evolution rates by isoprene-producing strains, however, points to an increased CEF. In line with our results, a previous study showed that the 1-IspS strain exhibited a decrease in linear electron transport compared to control strains, potentially linked to an observed decrease in light-harvesting pigments in the isoprene-producing strain (Rodrigues et al. 2023). Isoprene is also known for other biophysical and biochemical effects on cells and their membranes, such as a protective role in mitigating oxidative stress (Pollastri et al. 2019, reviewed in Pollastri et al. 2021), leading to reduced reductive power demands and thus a decrease in O_2 evolution. Upon short-term exposure to 40°C, both WT and isoprene-producing strains showed an increase in O_2 evolution (Figure 4C), which has been described before (Inoue et al. 2001), but no changes in the trend among the tested strains.

2.4 | Establishment and Quantification of Photosynthetic Isoprene Production by Optimised Strains in a Process-Relevant Photobioreactor Setup

To assess the performance of the best strains engineered in this study, that is, the strains carrying 2 (KJ26) and 3 (KJ27) *ispS* copies, in a process-relevant setup, we tested the strains in 3-L lab-scale stirred tank photobioreactors aerated with a gas mix of 5% CO_2 and 95% N_2 and operated in batch mode (Figure 5). For this purpose, 2 L of 2× BG11 medium without antibiotics were inoculated to an OD_{750} of 0.1 with seed cultures pre-acclimated to 2% CO_2. The light intensity was gradually increased from initially 100 to 1000 μmol photons $m^{-2}\,s^{-1}$ after 90 h (Figure 5A). O_2 partial pressure and CO_2 and O_2 concentrations in in- and off-gas were constantly monitored. For isoprene quantification, the off-gas was directly probed and analysed via GC (Figure 5C). While isoprene production by *Synechocystis* is known to be elevated at 40°C (Rodrigues et al. 2023), inoculation at 40°C was found to involve a long and unpredictable lag phase (not shown). Thus, a two-stage process was established, composed of a growth stage at 30°C to ensure swift biomass accumulation (white background in Figure 5), followed by a production phase at 40°C (grey background in Figure 5). Moreover, cultures were spiked every 48 h with nutrient mixes corresponding to a final concentration of 1× BG11 to ensure sufficient nutrient supply during the 40°C production phase (indicated by arrows in Figure 5). Growth rates in the initial exponential phase (0.10–0.11 h^{-1}) were comparable to those of *Synechocystis* WT in this cultivation system (0.13 h^{-1}). Exponential growth ended after 2–3 days, indicating light limitation (confirmed by an immediate increase of O_2 partial pressure upon light intensity increase, Figure S3), which persisted during the continued light intensity increase and led to gradually decreasing specific CO_2 uptake rates (Table 1, Figure S4) and apparently also a decrease of the specific isoprene production rates (Figure 5A). During operation at 30°C, the CO_2 share converted to isoprene was around 3% (Table 1).

After an OD_{750} of 10 was reached, the temperature was increased to 40°C, prompting an immediate increase in isoprene productivity with a CO_2 share converted to isoprene of around 23% (Table 1, Figure 5C1). At this stage, an isoprene productivity of around 51 μmol $L^{-1}\,h^{-1}$ (corresponding to 3.2 mg $L^{-1}\,h^{-1}$) was achieved (Figure 5B). Growth continued in this phase, and O_2 evolution increased immediately after the temperature increase (Figure 5C1), in accordance with O_2 evolution measurements on a small scale (Figure 4C).

After 48 h at 40°C, specific activity as well as O_2 partial pressure started to decline (Figure 5A). Given that a large amount of biomass had accumulated ($OD_{750} = 15$) and the process had been run for 7 days, the cells possibly faced nutrient limitation. Assuming a nitrogen content of 11.3% (g/g) in biomass (Shastri and Morgan 2005), corresponding to ~0.7 g of nitrogen for KJ26 and KJ27 at the measured OD_{750}, depletion of the nitrogen in the 2 L of 2× BG11 (0.528 g N) can be expected at this point. Thus, 30 mL of cell suspension were replaced with 30 mL of concentrated nutrient mix corresponding to the nutrient content of 2 L of 1× BG11 (black arrows in Figure 5).

14677652, 2026, 3, Downloaded from https://onlinelibrary.wiley.com/doi/10.1111/pbi.70395 by Uppsala University, Wiley Online Library on [27/05/2026]. See the Terms and Conditions (https://onlinelibrary.wiley.com/terms-and-conditions) on Wiley Online Library for rules of use; OA articles are governed by the applicable Creative Commons License

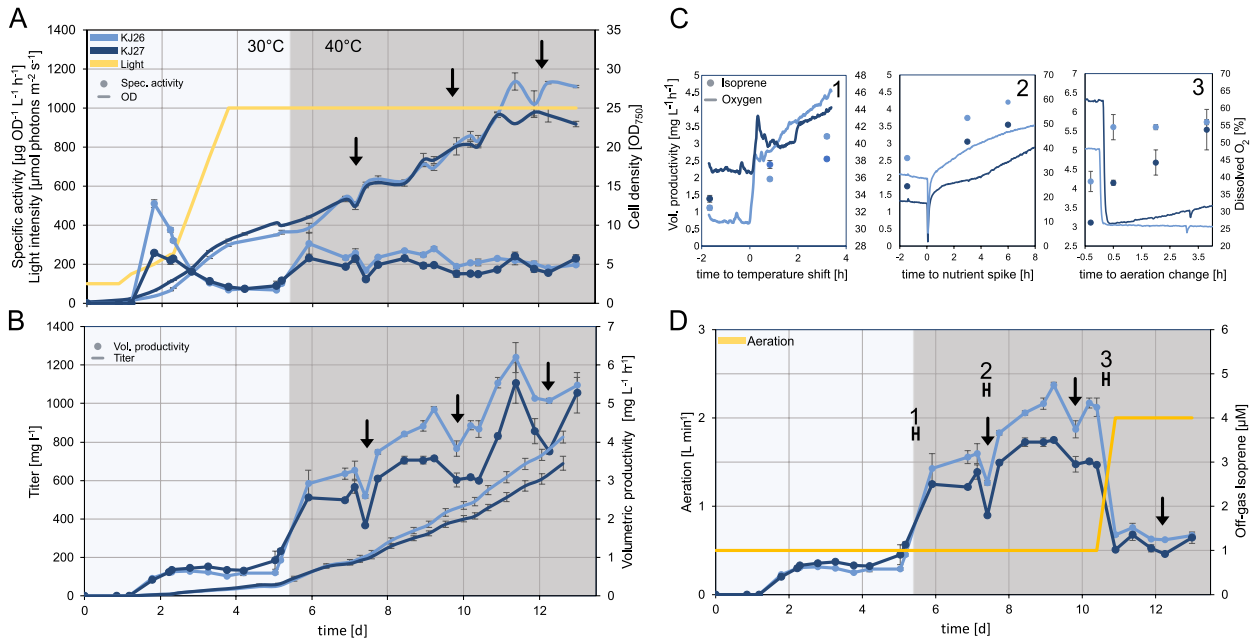

FIGURE 5 | Photosynthetic isoprene production using strains KJ26 and KJ27 in 2 L stirred tank photobioreactors. (A) Courses of cell concentrations (lines), specific isoprene production rates (lines with dots) and applied light intensity (yellow line). The specific activity was calculated by multiplication of the isoprene concentration in the off-gas with the aeration rate and division by the culture volume and cell density. (B) Courses of cumulative isoprene titres (lines) and isoprene productivities (lines with dots). Cumulative titres were calculated as the average of the volumetric productivity determined at the start and end of each interval, multiplied by the length of the interval for each time point. (C) Volumetric titres and dissolved O_2 levels during temperature shift (1), nutrient spike (2) and aeration change (3). (D) Aeration (yellow line) and isoprene concentration in the off-gas (lines with dots). Numbered are time intervals corresponding to graphs 1, 2 and 3 in panel C. Error bars correspond to standard deviations of at least technical duplicates. Arrows indicate spiking with concentrated nutrient mix corresponding to final concentrations in 1× BG11 medium. d, days; OD, OD_{750}; Spec. activity, specific activity.

This had an immediate effect on O_2 evolution as well as isoprene formation, suggesting that indeed certain nutrients were depleted (Figure 5C2). Intriguingly, this also enabled continuation of cell growth.

Given that previous studies on continuous isoprene production applied over 6 times higher aeration rates (Gao et al. 2016), aeration was increased from 0.5 to 2 L min^{-1} after 10 days (Figure 5D). This led to a lower isoprene concentration in the off-gas but increased isoprene productivity (Figure 5, panels D and C3). Average productivities of 5.48 and 4.60 mg L^{-1} h^{-1} were achieved over 3 days with KJ26 and KJ27, respectively, with a peak of up to 6.2 mg L^{-1} h^{-1} for KJ26 (Figure 5B). Overpressures in the reactor headspaces amounted to 37.6 (KJ27) and 30.9 (KJ26) mbar, ruling out that isoprene quantification was biased by pressure build-up. Possible reasons for the elevated isoprene productivity at higher aeration rates include more stringent product removal and thus less product inhibition and favourable thermodynamics. Moreover, the reduced O_2 partial pressure (Figure 5C3) might be favourable for high MEP pathway flux, considering the recently proposed role of the MEP pathway in detecting, signalling, and responding to oxidative stress (reviewed by Perez-Gil et al. 2024) and IspG and IspH both containing O_2-sensitive Fe-S clusters. Thus, isoprene formation in our small-scale tests may be affected by elevated, inhibitory O_2 concentrations and thus not reveal the true potential of production strains. This also may explain why KJ27, as the best-performing strain in small-scale tests, did not outcompete KJ26 in the bioreactor experiments. After 13 days, final cumulative titres of 0.83 and 0.69 g L^{-1} were achieved with KJ26 and KJ27, respectively.

It should be noted that, during the first 5 days at 30°C, less than 10% of the total isoprene was produced (Figure 5B), whereas more than 90%, 0.77 and 0.63 g L^{-1}, accumulated afterwards at 40°C and high cell concentrations in less than 8 days with KJ26 and KJ27, respectively. Moreover, given the stability of these isoprene producers (Figures 2 and 5A,B), it can be assumed that the process could have been prolonged and titres further increased. Nevertheless, the productivities achieved in this study are the highest ever reported for any photosynthetically produced terpenoid and approach the highest productivities reported for CO_2-based production with *Synechocystis*, that is, those achieved for 1-butanol and phenylpropanoids (Kukil et al. 2023; Liu et al. 2019, Table 2). Many factors, such as electron and precursor supply via host metabolism for the formation of the desired compound, product toxicity and the plasticity of and regulatory stringency for relevant pathways, greatly affect achievable productivities and titres. For instance, the natural ability of cyanobacteria to overproduce sugars to counteract desiccation and control osmotic pressure has been exploited to achieve very high titres (Lin et al. 2020), making use of native streamlining of metabolism via the conditions applied. In response to salt stress, isoprene production in *Synechocystis*, however, was shown to compete with compatible solute production (Pade et al. 2016). Circumventing native regulation of certain pathways thus has the potential to greatly improve performance. Adaptive laboratory evolution (ALE) constitutes a promising

14677652, 2026, 3, Downloaded from https://onlinelibrary.wiley.com/doi/10.1111/pbi.70395 by Uppsala University, Wiley Online Library on [27/05/2026]. See the Terms and Conditions (https://onlinelibrary.wiley.com/terms-and-conditions) on Wiley Online Library for rules of use; OA articles are governed by the applicable Creative Commons License

TABLE 1 | Process performance metrics in selected time intervals with closed carbon balance during isoprene production with *Synechocystis* strains in 2 L photobioreactors.

	Phase I [30°C]	Phase II [40°C]
	Carbon partitioning [%][a]	
KJ26	3.33	22.51
KJ27	3.72	23.37
	CO_2 uptake rate [mmol g_{CDW}^{-1} h^{-1}][a]	
KJ26	1.92	0.37
KJ27	1.74	0.24
	Specific activity [μmol min^{-1} g_{CDW}^{-1}][a]	
KJ26	0.23	0.29
KJ27	0.25	0.22
	Quantum yield [%][a,b]	
KJ26	1.08	3.26
KJ27	2.02	3.12

[a]Values were calculated for time intervals with closed carbon balance, i.e., less than 5% deviation among measured CO_2 uptake and summed up biomass and isoprene formation (KJ26 at 30°C: 55.08–90.33 h, KJ26 at 40°C: 164.95–244.55 h, KJ27 at 30°C: 42.92–55.08 h, KJ27 at 40°C: 177.83–272.92 h). CO_2 content of biomass was extrapolated from OD_{750} values via a OD_{750}-to-g_{CDW} L^{-1} correlation factor of 0.2% and 51% (wt/wt) carbon content of biomass (Shastri and Morgan 2005).
[b]Bioreactor surface area and applied light intensity were used to calculate quantum yields assuming that the production of one mole of isoprene consumes 56 mol of photons (Lan and Liao 2011).

approach to achieve this and simultaneously avoid complex phenotypes (Kukil et al. 2023). For example, ALE enabled the achievement of phenylpropanoid production on a gram-scale via dysregulation of host metabolism leading to improved precursor supply (Table 2). Selection for thermotolerant mutants may represent a promising basis for an ALE approach to improve isoprene production.

Isoprene and 1-butanol are comparable in terms of energy and carbon content. However, while isoprene formation only requires the introduction of isoprene synthase (Lindberg et al. 2010), 4 non-native genes had to be introduced into *Synechocystis* to produce 1-butanol from (R)-3-hydroxybutyryl-CoA. Given that these 1-butanol-forming enzymes efficiently draw carbon, extensive engineering of the surrounding carbon metabolism such as re-routing and elimination of competing pathways, further improved titres (Liu et al. 2019). In contrast, isoprene formation in plants is an auxiliary stress response that is not essential for survival, and thus isoprene synthases have evolved to not compete for precursors required for synthesis of essential terpenoids. As a result, all isoprene synthases characterised so far suffer from notoriously high K_m values and low turnover numbers, turning the final step of isoprene synthesis into a bottleneck with little to no effect when targeting other pathway enzymes or carbon metabolism (Figure 3). A potential solution to this problem may already exist in nature. Isoprene is the most abundant biogenic volatile organic hydrocarbon in the biosphere, and a wide range of organisms are emitting considerable amounts of isoprene (McGenity et al. 2018). Nevertheless, only a handful of isoprene synthases, all from terrestrial plants, have been identified so far. This leaves great potential for the discovery of more efficient enzymes from hosts that may resemble cyanobacteria more closely.

Compared to the current benchmark study for cyanobacterial isoprene production, which achieved a 3-day average space–time yield of up to 4.7 mg L^{-1} h^{-1} and a titre of 1.26 g L^{-1} of isoprene in 21 days with an *S. elongatus* strain (Gao et al. 2016), a similar isoprene production performance was achieved in this study. The approach taken however differed in several aspects. First, overexpression of biosynthetic genes in the best-performing strain of that benchmark study was driven by IPTG induction, which is not applicable for scale-up. Moreover, the applied 55 mL custom-made bioreactors with 25 mL volume were aerated with 4.8 L h^{-1} corresponding to a VVM (volume of air sparged per volume of liquid per min) of 3.2. In this study, a maximal VVM of 1 in a 2 L photobioreactor was applied, and the aeration rate was found to be a key factor influencing bioprocess performance. A further increase in aeration rate might improve isoprene space–time yields, but isoprene concentration in the off-gas then becomes diluted, complicating product isolation. Lastly, *S. elongatus* thrives at higher temperatures compared to *Synechocystis* and thus might be more suitable for isoprene production in general. This is also illustrated by the fact that the currently best-performing isoprene synthase of *E. globulus* can be stably expressed in *S. elongatus*, while overexpression of this enzyme in *Synechocystis* or *E. coli* required co-expression of either Dxs or Idi (Englund et al. 2018; Volke et al. 2019), pointing towards a more favourable precursor supply in *S. elongatus* and thus a better suitability of this strain for isoprene production.

The volumetric productivities achieved here are still far off from the currently best heterotrophic process in which *E. coli* reaches up to 2 g L^{-1} h^{-1} with a mass yield of 10.7% for the conversion of glucose to isoprene (Whited et al. 2010). However, a fair comparison should consider the surface area needed for production of the carbon source, which relies on a photosynthetic process. Thus, when considering the surface area required for sugar production based on sugar cane (Brandenburg et al. 2021) and a mass yield of 10.7% for the conversion of glucose to isoprene, the currently best heterotrophic process yields 1.13 t ha^{-1} a^{-1}. Assuming a large-scale photobioreactor with a volume of 750 000 L ha^{-1} (Nilsson et al. 2020), 12 h of sunlight per day, 6 months downtime in winter and the highest 3-day average productivity achieved in the bioreactor experiment (5.48 mg L^{-1} h^{-1}), an isoprene production of 9.00 t ha^{-1} a^{-1} could be reached, not taking into account that the cyanobacterial process does neither require arable land nor compete with food production. Thus, in terms of land use efficiency, a crucial metric when assessing the potential of a process to drive the bioeconomy of the future, the phototrophic process developed in this study is about 8 times more efficient than the currently best heterotrophic system making use of renewable resources.

The productivities achieved here relied all on artificial light sources with high intensity. To assess whether a similar performance could be achieved with sunlight, the quantum yield of the process and the available solar irradiance have to be taken into account. While initially at 1%–2%, the photon usage efficiency, i.e., the amount of isoprene produced per

14677652, 2026, 3, Downloaded from https://onlinelibrary.wiley.com/doi/10.1111/pbi.70395 by Uppsala University, Wiley Online Library on [27/05/2026]. See the Terms and Conditions (https://onlinelibrary.wiley.com/terms-and-conditions) on Wiley Online Library for rules of use; OA articles are governed by the applicable Creative Commons License

TABLE 2 | Comparison of highest C-based productivities reported for CO_2-derived products with diverse cyanobacterial hosts.

Host	Product	Cmmol L^{-1} day^{-1}	System	Source
PCC 6803	Acetone	0.62	Shake flask	Zhou et al. (2012)
	Bisabolene	1.37	High-density cultivation (CellDEG)	Rodrigues and Lindberg (2021b)
	1-Butanol	16.30	Plug-sealed tissue culture flasks	Liu et al. (2019)
	Trans-cinnamic acid	16.95	High-density cultivation (CellDEG)	Kukil et al. (2023)
	p-coumaric acid	15.21	High-density cultivation (CellDEG)	Kukil et al. (2023)
	Ethanol	9.21	400 mL column photobioreactor	Gao et al. (2012)
	Ethylene	12.19	Shake flask	Ungerer et al. (2012)
	Fatty acids	0.72	Shake flask	Liu et al. (2011)
	Fatty alcohols	0.01	Shake flask	Yao et al. (2014)
	Isobutanol	2.35	Plug-sealed tissue culture flasks	Miao et al. (2018)
	Isoprene	**9.66**	**2 L stirred tank PBR**	**This study**
	D-lactate	8.83	Shake flask	Zhou et al. (2014)
	L-lactate	1.99	Shake flask	Angermayr et al. (2014)
	Methyl laurate	1.99	Shake flask	Yunus et al. (2020)
	Squalene	0.018	Bubbled flask	Englund et al. (2014)
PCC 7120	*Limonene*	0.01	Shake flask	Halfmann et al. (2014)
PCC 7942	2,3-Butanediol	5.05	Shake flask	Oliver et al. (2013)
	1-Butanol	0.08	Shake flask	Lan and Liao (2012)
	Isobutanol	4.05	Aerated Roux culture bottles	Atsumi et al. (2009)
	Isobutyraldehyde	8.29	Aerated Roux culture bottles	Atsumi et al. (2009)
	Isoprene	7.50	55 mL custom-designed photobioreactor	Gao et al. (2016)
	2-Methyl-1-butanol	1.13	Screw-cap flasks	Shen and Liao (2012)
PCC 7002	*Bisabolene*	0.01	Shake flask	Davies et al. (2014)
	Fatty acids	0.42	Aerated bottle	Ruffing (2014)
	Limonene	0.07	Shake flask	Davies et al. (2014)
	Mannitol	4.94	Bubbled flask	Jacobsen and Frigaard (2014)
PCC 11901	Free fatty acids	19.22	Shake flask	Włodarczyk et al. (2020)
PCC 11801	Ethylene	0.04	Multicultivator MC-1000-OD	Sengupta et al. (2020)
	Succinate	6.30	Multicultivator MC-1000-OD	Sengupta et al. (2020)
UTEX 2973	Cadaverine	0.68	Shake flask	Dookeran and Nielsen (2021)
	Glutarate	0.64	Shake flask	Dookeran and Nielsen (2021)
	Inositol	1.25	Shake flask/Shaking photoincubator	Sun et al. (2023)
	Limonene	0.60	Shake flask	Lin et al. (2021)
	Sucrose	70.12	Shake flask	Lin et al. (2020)

Note: For mixed products, such as fatty acids, the most abundantly produced compound was used for calculation. Numbers are rounded up to two decimal digits. From this study, the average productivity achieved in the last 3 days of the bioreactor experiments is given. Terpenoids are given in italics. Productivities achieved in this study is given in bold.

14677652, 2026, 3, Downloaded from https://onlinelibrary.wiley.com/doi/10.1111/pbi.70395 by Uppsala University, Wiley Online Library on [27/05/2026]. See the Terms and Conditions (https://onlinelibrary.wiley.com/terms-and-conditions) on Wiley Online Library for rules of use; OA articles are governed by the applicable Creative Commons License

incumbent photon, reached over 3% during the 40°C production phase (Table 1) with peak values of up to 5.26%, based on the assumption that generating 1 mol of isoprene requires 56 mol of photons, considering the NADPH and ATP necessary for CO_2 fixation and isoprene synthesis (Lan and Liao 2011). This corresponds to an energy requirement of 9716 kJ per mol of isoprene, assuming an average energy of 173.5 kJ mol^{-1} for 680–700 nm photons. Thus, with an average annual solar energy on earth of 6.32×10^6 kJ m^{-2} a^{-1} (Lan and Liao 2011) and a photon use efficiency of 3%, 1.33 kg m^{-2} a^{-1} of isoprene could be produced with average sunlight, which is in the same range as what has been achieved experimentally in this study (1.02 kg m^{-2} a^{-1}). Thus, natural sunlight should provide sufficient energy to achieve similar volumetric productivities in outdoor settings.

3 | Conclusions

4th-generation biofuels and renewable chemicals, such as photosynthetically generated isoprene, are a key cornerstone en route to the bioeconomy of the future. The technoeconomic feasibility of underlying processes is, however, often not given due to the inefficiency and instability of the engineered cell factories. In this study, we have developed a markerless platform strain, demonstrating a stable isoprene production phenotype for over half a year without selection pressure. Probing the upstream carbon metabolism and the MEP pathway of the platform strain for bottlenecks, we identified isoprene synthase as a major limiting factor that was relieved by introducing a second isoprene synthase gene copy. When tested in process-relevant photobioreactor experiments, the resulting strains showed the highest reported production rates for any photosynthetically generated terpenoid. The results reported here represent a stepping stone towards the implementation of cyanobacterial photobiotechnology.

4 | Experimental Procedures

4.1 | Strains and Growth Conditions

E. coli strain DH5αZ1 (Expressys, Bammental, Germany) was used for subcloning and cultivated at 37°C in liquid LB medium with respective antibiotics (chloramphenicol 35 μg mL^{-1} or erythromycin 200 μg mL^{-1}). *Synechocystis* strains were grown in 6-well plates from cryo-stocks in BG11 with respective antibiotics (kanamycin 50 μg mL^{-1}, chloramphenicol 35 μg mL^{-1}, erythromycin 50 μg mL^{-1}) at 15 μmol photons m^{-2} s^{-1} and 30°C. Main cultures were grown in 100 mL Erlenmeyer flasks in the same media at 30°C and 50 μmol photons m^{-2} s^{-1}. The isoprene-producing base strain 1-IspS that was used for all further engineering was generated in a previous study (Rana et al. 2022). All *Synechocystis* PCC 6803 strains used and generated in this study are given in Table S1.

4.2 | Plasmid Construction

All PCR primers used in this study are given in Table S2. For the deletion of the kanamycin resistance cassette from strain 1-IspS, the CRISPR-Cas12 plasmid pSL2680 (Ungerer and Pakrasi 2016) was used. The antibiotic resistance of pSL2680 was changed from kanamycin to chloramphenicol using HiFi DNA Assembly Master Mix (NEB) from three PCR products (priKJ05/06, priKJ07/08, priKJ09/10), resulting in the plasmid pKJ04. Annealed oligos (priKJ16, priKJ17) were ligated into the AarI sites of pKJ04 as gRNA targeting the kanamycin resistance cassette, resulting in the new plasmid pKJ05. The homology repair cassette was generated via overlap-extension PCR from two fragments generated with primers priKJ18/19 and priKJ20/21 and ligated into the BamHI, KpnI site of pKJ05, resulting in pKJ06.

For *Eg-ispS* overexpression from the *phaAB* locus, plasmid phaAB_*Eg-IspS* was generated via AQUA cloning (Beyer et al. 2015). Here, the origin of replication of pEERM3 was fused to 500 bp of the *phaAB* up- and downstream region, a chloramphenicol resistance cassette and the Ptrc-RiboJ-*Eg-ispS* expression cassette using pEERM3_2MEP-IspS2 as a template (Rana et al. 2022). Plasmids for control knockout of *phaAB* were generated by amplification of phaAB_*Eg-IspS* with 5′-phosphorylated primers 5′P_CmR_fw/5′P_PhaABup_rev, DpnI digestion and subsequent ligation. For overexpression of *Eg-ispS* from the *ddh* site, the Ptrc-RiboJ-*Eg-IspS* expression cassette was amplified from phaAB_*Eg-IspS* using primers PhaABup_IspS_fw/IspS-CmR_rev and fused to a backbone containing an erythromycin resistance cassette and *ddh* 1 kb upstream and downstream region generated via PCR. The ddh:EmR knockout plasmid was generated from plasmid *ddh_Eg-ispS* via PCR (priKJ176/177), DpnI digestion and ligation, resulting in pKJ45.

For construction of the *Pt-ispH* and *Rc-ispH* expression constructs, the sequences used by Bongers et al. 2020 (GenBank ID MH605329 and MH605331, respectively) with truncations of the chloroplast targeting peptides were codon optimised for expression in *Synechocystis* and synthesised (Invitrogen/ThermoFisher Scientific, Waltham, USA). The insertion fragment was generated via overlap-extension PCR from three fragments (Ptrc-HIS priKJ80/22, *Pt-ispH* priKJ28/82 or *Rc-ispH* priKJ32/84, *ispG*-FLAG priKJ83/81) and ligated into the pEERM_phaAB (*phaAB:Eg-ispS*) backbone XbaI and PstI sites, generating plasmids pKJ14 and pKJ15. The construct for *cp12* insertions was generated using AQUA cloning (Beyer et al. 2015) and HiFi DNA Assembly from four (*cp12:CmR*) and five (*cp12:Eg-ispS*) fragments generated by PCRs, consisting of the pEERM backbone, 700 bp homology arms upstream and downstream of the *cp12* coding sequence, the chloramphenicol resistance and the Ptrc-RiboJ:*Eg-ispS* expression cassette (*cp12:Eg-ispS* priKJ1112/113, priKJ114/115, priKJ116/117, priKJ118/119, priKJ120/121; *cp12:CmR* priKJ112/113, priKJ114/115, priKJ119/116, priKJ120/121), resulting in pKJ23 and pKJ22. priKJ112/113, priKJ114/115, priKJ119/116, priKJ120/121, resulting in pKJ23 and pKJ22.

4.3 | Introduction of Gene Constructs Into *Synechocystis*

The previously published 1-IspS ('IspS') strain (Rana et al. 2022) was used as the starting strain for the implementation of

14677652, 2026, 3, Downloaded from https://onlinelibrary.wiley.com/doi/10.1111/pbi.70395 by Uppsala University, Wiley Online Library on [27/05/2026]. See the Terms and Conditions (https://onlinelibrary.wiley.com/terms-and-conditions) on Wiley Online Library for rules of use; OA articles are governed by the applicable Creative Commons License

further genetic modifications. The CRISPR-Cas12 plasmid pKJ06 was introduced into 1-IspS by triparental mating using the *E. coli* HB101 strain carrying the pRL443 conjugative plasmid (Elhai and Wolk 1988). Selection was carried out on BG11 plates with chloramphenicol at 50 μg mL^{-1}. Single colonies were picked, and the deletion of the kanamycin resistance cassette was confirmed by colony PCR and the inability to grow on BG11 supplemented with kanamycin. To cure the CRISPR-Cas12 plasmid, cells were grown in liquid BG11 medium without antibiotics and spread on BG11 agar plates without antibiotics to select individual colonies for restreaking onto BG11 agar plates without antibiotics and plates supplemented with chloramphenicol at 35 μg mL^{-1}. Colonies unable to grow on chloramphenicol were selected and preserved as KJ-05.

Subsequent genetic modifications were generated by double homologous recombination via natural transformation (Liu et al. 2019). *Synechocystis* cultures were grown to the early linear growth phase (OD_{750} = 0.3–0.6), and cells were collected by centrifugation. 1–2 μg of plasmid DNA was added to 200 μL of concentrated cell suspension and incubated for 4–6 h under standard conditions (50 μmol photons m^{-2} s^{-1} illumination and 30°C). Cells were spread on nitrocellulose membranes (0.45 μm, Cat. No. 10401672, Cytiva, Marlborough, USA) on BG11 agar plates without antibiotics and incubated under standard conditions for 18–24 h, before the filters were transferred to BG11 plates with respective antibiotics (35 μg mL^{-1} chloramphenicol, 50 μg mL^{-1} erythromycin). Single colonies were streaked onto BG11 plates with antibiotics and analysed by colony PCR. Positive transformants were cultivated in liquid BG11 with antibiotics in 6-well plates before cultivation in 100 mL Erlenmeyer flasks, all under standard conditions. Before cryopreservation of the strains, segregation was confirmed via PCR. For preparation of genomic DNA templates, 200–500 μL of liquid cultures were harvested at an OD_{750} of 0.5–2.0 via centrifugation and cells were resuspended in 100 μL TE buffer (19 mM TRIS, 1 mM EDTA, pH 8.0) supplemented with 0.05% triton X-100.

4.4 | Assessment of Isoprene Production

Isoprene-producing strains were seeded to OD_{750} = 0.1 into 25 mL BG11 without antibiotics (pH adjusted to 8.0 with 100 mM TES) in 100 mL Erlenmeyer flasks and grown for three days with 50 μmol photons m^{-2} s^{-1} illumination at 30°C and 120 rpm on an orbital shaker. After three days (if not indicated otherwise), the cultures were transferred to incubators operated at 120 μmol photons m^{-2} s^{-1}, 40°C and 150 rpm for at least one hour. Optical density was determined and 20 mL of each culture adjusted to OD_{750} = 0.5 was transferred to cylindrical 60 mL gas chromatography (GC) vials (Fisherbrand cat. no. 11540585) and supplemented with 50 mM of sodium bicarbonate. Cultures were incubated again at 120 μmol photons m^{-2} s^{-1} illumination at 40°C for 30–120 min at 150 rpm on an orbital shaker. For each strain, three to four biological replicates derived from a single colony were analysed. From the cultures incubated in GC vials for 30–120 min, 150 μL of headspace gas was injected in a Clarus 580 (Perkin Elmer, Waltham, USA) gas chromatograph (GC) equipped with a flame-ionisation detector (FID) and a Porapak QS packed column (Porapak QS 80/80 PE 8000, 1.8 m × 2 mm ID, Cat. No. N9305013-ZW5531, Perkin Elmer). The oven temperature was 200°C for 2.5 min, and the carrier gas was N_2 at 20 mL min^{-1}. Isoprene elution peaked at 1.74 min and was quantified based on the peak area and synthetic standards. OD_{750} was determined after sampling. For protein analysis, cell pellets from production experiments were frozen at −80°C.

4.5 | Protein Detection

Frozen *Synechocystis* cell pellets were resuspended in 200 μL TBS buffer (20 mM Tris base, 150 mM NaCl) and thawed at 37°C. EDTA (5 mM) and 2 μL ProteaseArrest (G-Bioscience, St. Louis, USA) were added. After the addition of 0.1 mm glass beads, cells were physically disrupted with four cycles of 30 s at 5500 rpm using a bead-beater. Supernatant was collected as crude cell lysate, and protein content was quantified by DC protein assay (BIO-RAD, Hercules, USA). Different amounts of protein were loaded depending on the protein tag: 5 μg for strep-tag, 20 μg for flag-tag, 30 μg for his-tag and 10 μg for AtpB-based detection. After separation and blotting, detection of the proteins was performed using primary anti-strep-tag antibody (AB76950, AbCam, Cambridge, UK), anti-flag-tag antibody (F3165, Sigma-Aldrich, St. Louis, USA), anti-his-tag antibody (A00186, Genscript, Piscataway, USA), anti-AtpB antibody (AS05085, Agrisera, Vännäs, Sweden) and secondary anti-rabbit (A5101114, Agrisera) and anti-mouse (A509627, Agrisera) antibodies. The AtpB antibody was used as a loading control for semi-quantitative analysis of *ispS* expression in different strains. For semi-quantitative Western blot analysis, the band intensity of AtpB and Flag-IspS signals was measured in technical triplicates. The IspS signal of each strain was normalised to its AtpB signal to obtain the relative IspS expression level in each strain. Subsequently, relative IspS expression levels were normalised to the level in strain KJ05.

4.6 | O_2 Evolution Experiment and Chlorophyll Extraction

Specific O_2 evolution rates of *Synechocystis* strains were assessed using a Clark-type electrode (Hansatech Electrode Disc S1, Hansatech, Norfolk, UK). Prior to the measurements, the electrode was calibrated with air-saturated water and the addition of sodium dithionite at either 30 or 40°C. *Synechocystis* cultures were cultivated at 50 μmol photons m^{-2} s^{-1} and 30°C. For O_2 evolution measurements at 40°C, cultures were pre-incubated at 40°C for at least 30 min. All *Synechocystis* cultures were pre-incubated in darkness for at least 30 min. 1.0 mL of *Synechocystis* culture and 20 mM of sodium bicarbonate were added to the Clark cell in darkness. O_2 consumption was measured for 5 min in darkness. Subsequently, O_2 evolution was measured under saturated light conditions. The corrected maximal O_2 evolution rate was calculated with the averaged O_2 consumption rate in darkness added to the averaged maximal O_2 evolution rate in saturated light conditions and subsequently normalised to the chlorophyll a content. Chlorophyll a content were determined for each sample via extraction using 80% acetone and measuring absorbance at 663.6, 646.6 and 750 nm (Porra et al. 1989; Yang et al. 1998).

14677652, 2026, 3, Downloaded from https://onlinelibrary.wiley.com/doi/10.1111/pbi.70395 by Uppsala University, Wiley Online Library on [27/05/2026]. See the Terms and Conditions (https://onlinelibrary.wiley.com/terms-and-conditions) on Wiley Online Library for rules of use; OA articles are governed by the applicable Creative Commons License

4.7 | Isoprene Production in Photobioreactors

For isoprene production in lab-scale photobioreactors, seed cultures were inoculated in 100 mL 2× BG11 in 500 mL baffled Erlenmeyer flasks to an OD_{750} of 0.1 and cultivated at 50 µmol photons $m^{-2}s^{-1}$, 30°C, 75% humidity and 2% CO_2 for a week. Before inoculation of the stirred tank photobioreactors (Labfors 5 Lux, Infors, Switzerland), 2 L of 2× BG11 were saturated with 5% CO_2 and pH was stabilised overnight. Pressures in the reactor headspace and off-gas line were measured using a digital manometer (CPG1200, Wika, Germany). Bioreactors were inoculated to an OD_{750} of 0.1 and operated at an initial light intensity of 100 µmol photons $m^{-2}s^{-1}$, 300 rpm, 30°C, pH 7.4, and 0.5 L min^{-1} aeration with a gas mix consisting of 5% CO_2 and 95% N_2. The light intensity was gradually increased over time, finally reaching 1000 µmol photons $m^{-2}s^{-1}$. After 6 days, the temperature was increased to 40°C. After the temperature increase, a concentrated nutrient solution corresponding to 1× BG11 of the reactor volume was added every 48 h. Isoprene was directly sampled from the off-gas using custom-made bubble traps or by flushing 10 mL GC vials with off-gas. CO_2 and O_2 in in- and off-gas were monitored with BlueInOne Cell gas analysers (BlueSens, Germany). CO_2 consumption was calculated by multiplying the discrepancy in CO_2 percentage in in- and off-gas with the air flow rate. For the calculation of total carbon in biomass, a biomass carbon content of 51% (g/g) was assumed (Shastri and Morgan 2005). Bioreactor surface area and applied light intensity were used to calculate quantum yields, assuming that the production of one mole of isoprene consumes 56 mol of photons (Lan and Liao 2011).

Author Contributions

Conceptualization and study design: K.N.J., P.B., P.L.; Experimental work and data collection: K.N.J., P.B., A.T., J.T., D.S.; Data curation and interpretation: K.N.J., P.B., P.L., B.B.; P.B. and K.N.J. wrote the original draft of the manuscript; all authors contributed to article structuring and editing and all authors have given approval to the final version of the manuscript.

Conflicts of Interest

The authors declare no conflicts of interest.

Data Availability Statement

All data and results are presented in the paper and in the Supporting Information. Raw data will be made available upon request to pia.lindberg@kemi.uu.se.

References

Angermayr, S. A., A. D. van der Woude, D. Correddu, A. Vreugdenhil, V. Verrone, and K. J. Hellingwerf. 2014. "Exploring Metabolic Engineering Design Principles for the Photosynthetic Production of Lactic Acid by *Synechocystis* sp. PCC6803." *Biotechnology for Biofuels* 7: 99. https://doi.org/10.1186/1754-6834-7-99.

Atsumi, S., W. Higashide, and J. C. Liao. 2009. "Direct Photosynthetic Recycling of Carbon Dioxide to Isobutyraldehyde." *Nature Biotechnology* 27: 1177–1180. https://doi.org/10.1038/nbt.1586.

Bae, J. Y., J. Laplaza, and T. W. Jeffries. 2008. "Effects of Gene Orientation and Use of Multiple Promoters on the Expression of XYL1 and XYL2 in *Saccharomyces cerevisiae*." *Applied Biochemistry and Biotechnology* 145: 69–78. https://doi.org/10.1007/s12010-007-8076-0.

Banerjee, A., Y. Wu, R. Banerjee, Y. Li, H. Yan, and T. D. Sharkey. 2013. "Feedback Inhibition of Deoxy-D-Xylulose-5-Phosphate Synthase Regulates the Methylerythritol 4-Phosphate Pathway." *Journal of Biological Chemistry* 288: 16926–16936. https://doi.org/10.1074/jbc.M113.464636.

Behler, J., D. Vijay, W. R. Hess, and M. K. Akhtar. 2018. "CRISPR-Based Technologies for Metabolic Engineering in Cyanobacteria." *Trends in Biotechnology* 36: 996–1010. https://doi.org/10.1016/j.tibtech.2018.05.011.

Beyer, H. M., P. Gonschorek, S. L. Samodelov, M. Meier, W. Weber, and M. D. Zurbriggen. 2015. "AQUA Cloning: A Versatile and Simple Enzyme-Free Cloning Approach." *PLoS One* 10: e0137652. https://doi.org/10.1371/journal.pone.0137652.

Blanc-Garin, V., T. Veaudor, P. Sétif, et al. 2022. "First In Vivo Analysis of the Regulatory Protein CP12 of the Model Cyanobacterium *Synechocystis* PCC 6803: Biotechnological Implications." *Frontiers in Plant Science* 13: 999672.

Bolay, P., N. Dodge, K. Janssen, P. E. Jensen, and P. Lindberg. 2024. "Tailoring Regulatory Components for Metabolic Engineering in Cyanobacteria." *Physiologia Plantarum* 176: e14316. https://doi.org/10.1111/ppl.14316.

Bongers, M., J. Perez-Gil, M. P. Hodson, et al. 2020. "Adaptation of Hydroxymethylbutenyl Diphosphate Reductase Enables Volatile Isoprenoid Production." *eLife* 9: e48685. https://doi.org/10.7554/eLife.48685.

Borowitzka, M. A., and A. Vonshak. 2017. "Scaling Up Microalgal Cultures to Commercial Scale." *European Journal of Phycology* 52: 407–418. https://doi.org/10.1080/09670262.2017.1365177.

Brandenburg, F., E. Theodosiou, C. Bertelmann, et al. 2021. "*Trans*-4-Hydroxy-L-Proline Production by the Cyanobacterium *Synechocystis* sp. PCC 6803." *Metabolic Engineering Communications* 12: e00155. https://doi.org/10.1016/j.mec.2020.e00155.

Camsund, D., T. Heidorn, and P. Lindblad. 2014. "Design and Analysis of LacI-Repressed Promoters and DNA-Looping in a Cyanobacterium." *Journal of Biological Engineering* 8: 4. https://doi.org/10.1186/1754-1611-8-4.

Čelešnik, H., A. Tanšek, A. Tahirović, et al. 2016. "Biosafety of Biotechnologically Important Microalgae: Intrinsic Suicide Switch Implementation in Cyanobacterium *Synechocystis* sp. PCC 6803." *Biology Open* 5: 519–528. https://doi.org/10.1242/bio.017129.

Chaves, J. E., and A. Melis. 2018. "Biotechnology of Cyanobacterial Isoprene Production." *Applied Microbiology and Biotechnology* 102: 6451–6458. https://doi.org/10.1007/s00253-018-9093-3.

Cid Gomes, L., S. Vajravel, W. Siljebo, et al. 2025. "Multiliter-Scale Photosensitized Dimerization of Isoprene to Sustainable Aviation Fuel Precursors." *ACS Sustainable Chemistry & Engineering* 13: 2467–2476. https://doi.org/10.1021/acssuschemeng.4c08755.

Davies, F. K., V. H. Work, A. S. Beliaev, and M. C. Posewitz. 2014. "Engineering Limonene and Bisabolene Production in Wild Type and a Glycogen-Deficient Mutant of *Synechococcus* sp. PCC 7002." *Frontiers in Bioengineering and Biotechnology* 2: 21. https://doi.org/10.3389/fbioe.2014.00021.

Demoulin, C. F., Y. J. Lara, L. Cornet, et al. 2019. "Cyanobacteria Evolution: Insight From the Fossil Record." *Free Radical Biology & Medicine* 140: 206–223. https://doi.org/10.1016/j.freeradbiomed.2019.05.007.

Di, X., D. Ortega-Alarcon, R. Kakumanu, et al. 2023. "MEP Pathway Products Allosterically Promote Monomerization of Deoxy-D-Xylulose-5-Phosphate Synthase to Feedback-Regulate Their Supply." *Plant Communications* 4: 100512. https://doi.org/10.1016/j.xplc.2022.100512.

14677652, 2026, 3, Downloaded from https://onlinelibrary.wiley.com/doi/10.1111/pbi.70395 by Uppsala University, Wiley Online Library on [27/05/2026]. See the Terms and Conditions (https://onlinelibrary.wiley.com/terms-and-conditions) on Wiley Online Library for rules of use; OA articles are governed by the applicable Creative Commons License

Dookeran, Z. A., and D. R. Nielsen. 2021. "Systematic Engineering of *Synechococcus elongatus* UTEX 2973 for Photosynthetic Production of l-Lysine, Cadaverine, and Glutarate." *ACS Synthetic Biology* 10: 3561–3575. https://doi.org/10.1021/acssynbio.1c00492.

Elhai, J., and C. P. Wolk. 1988. "Conjugal Transfer of DNA to Cyanobacteria." *Methods in Enzymology* 167: 747–754. https://doi.org/10.1016/0076-6879(88)67086-8.

Englund, E., J. Andersen-Ranberg, R. Miao, B. Hamberger, and P. Lindberg. 2015. "Metabolic Engineering of *Synechocystis* sp. PCC 6803 for Production of the Plant Diterpenoid Manoyl Oxide." *ACS Synthetic Biology* 4: 1270–1278. https://doi.org/10.1021/acssynbio.5b00070.

Englund, E., B. Pattanaik, S. J. K. Ubhayasekera, K. Stensjö, J. Bergquist, and P. Lindberg. 2014. "Production of Squalene in *Synechocystis* sp. PCC 6803." *PLoS One* 9: e90270. https://doi.org/10.1371/journal.pone.0090270.

Englund, E., K. Shabestary, E. P. Hudson, and P. Lindberg. 2018. "Systematic Overexpression Study to Find Target Enzymes Enhancing Production of Terpenes in *Synechocystis* PCC 6803, Using Isoprene as a Model Compound." *Metabolic Engineering* 49: 164–177. https://doi.org/10.1016/j.ymben.2018.07.004.

Gao, X., F. Gao, D. Liu, H. Zhang, X. Nie, and C. Yang. 2016. "Engineering the Methylerythritol Phosphate Pathway in Cyanobacteria for Photosynthetic Isoprene Production From CO_2." *Energy & Environmental Science* 9: 1400–1411. https://doi.org/10.1039/C5EE03102H.

Gao, Z., H. Zhao, Z. Li, X. Tan, and X. Lu. 2012. "Photosynthetic Production of Ethanol From Carbon Dioxide in Genetically Engineered Cyanobacteria." *Energy & Environmental Science* 5: 9857–9865. https://doi.org/10.1039/C2EE22675H.

Halfmann, C., L. Gu, and R. Zhou. 2014. "Engineering Cyanobacteria for the Production of a Cyclic Hydrocarbon Fuel From CO_2 and H_2O." *Green Chemistry* 16: 3175–3185. https://doi.org/10.1039/C3GC42591F.

Inoue, N., Y. Taira, T. Emi, et al. 2001. "Acclimation to the Growth Temperature and the High-Temperature Effects on Photosystem II and Plasma Membranes in a Mesophilic Cyanobacterium, *Synechocystis* sp. PCC6803." *Plant and Cell Physiology* 42: 1140–1148. https://doi.org/10.1093/pcp/pce147.

Jacobsen, J. H., and N.-U. Frigaard. 2014. "Engineering of Photosynthetic Mannitol Biosynthesis From CO_2 in a Cyanobacterium." *Metabolic Engineering* 21: 60–70. https://doi.org/10.1016/j.ymben.2013.11.004.

Jones, P. R. 2014. "Genetic Instability in Cyanobacteria – An Elephant in the Room?" *Frontiers in Bioengineering and Biotechnology* 2: 12. https://doi.org/10.3389/fbioe.2014.00012.

Knoop, H., and R. Steuer. 2015. "A Computational Analysis of Stoichiometric Constraints and Trade-Offs in Cyanobacterial Biofuel Production." *Frontiers in Bioengineering and Biotechnology* 3: 47. https://doi.org/10.3389/fbioe.2015.00047.

Koch, M., K. W. Berendzen, and A. K. Forchhammer. 2020. "On the Role and Production of Polyhydroxybutyrate (PHB) in the Cyanobacterium *Synechocystis* sp. PCC 6803." *Life (Basel)* 10: E47. https://doi.org/10.3390/life10040047.

Kukil, K., E. Englund, N. Crang, E. P. Hudson, and P. Lindberg. 2023. "Laboratory Evolution of *Synechocystis* sp. PCC 6803 for Phenylpropanoid Production." *Metabolic Engineering* 79: 27–37. https://doi.org/10.1016/j.ymben.2023.06.014.

Lan, E. I., and J. C. Liao. 2011. "Metabolic Engineering of Cyanobacteria for 1-Butanol Production From Carbon Dioxide." *Metabolic Engineering* 13: 353–363. https://doi.org/10.1016/j.ymben.2011.04.004.

Lan, E. I., and J. C. Liao. 2012. "ATP Drives Direct Photosynthetic Production of 1-Butanol in Cyanobacteria." *Proceedings of the National Academy of Sciences of the United States of America* 109: 6018–6023. https://doi.org/10.1073/pnas.1200074109.

Lichtenthaler, H. K. 1999. "The 1-Deoxy-D-Xylulose-5-Phosphate Pathway of Isoprenoid Biosynthesis in Plants." *Annual Review of Plant Physiology and Plant Molecular Biology* 50: 47–65. https://doi.org/10.1146/annurev.arplant.50.1.47.

Lin, P.-C., F. Zhang, and H. B. Pakrasi. 2020. "Enhanced Production of Sucrose in the Fast-Growing Cyanobacterium *Synechococcus elongatus* UTEX 2973." *Scientific Reports* 10: 390. https://doi.org/10.1038/s41598-019-57319-5.

Lin, P.-C., F. Zhang, and H. B. Pakrasi. 2021. "Enhanced Limonene Production in a Fast-Growing Cyanobacterium Through Combinatorial Metabolic Engineering." *Metabolic Engineering Communications* 12: e00164. https://doi.org/10.1016/j.mec.2021.e00164.

Lindberg, P., S. Park, and A. Melis. 2010. "Engineering a Platform for Photosynthetic Isoprene Production in Cyanobacteria, Using *Synechocystis* as the Model Organism." *Metabolic Engineering* 12: 70–79. https://doi.org/10.1016/j.ymben.2009.10.001.

Liu, H., Y. Sun, K. R. M. Ramos, et al. 2013. "Combination of Entner-Doudoroff Pathway With MEP Increases Isoprene Production in Engineered *Escherichia coli*." *PLoS One* 8: e83290. https://doi.org/10.1371/journal.pone.0083290.

Liu, X., R. Miao, P. Lindberg, and P. Lindblad. 2019. "Modular Engineering for Efficient Photosynthetic Biosynthesis of 1-Butanol From CO_2 in Cyanobacteria." *Energy & Environmental Science* 12: 2765–2777. https://doi.org/10.1039/C9EE01214A.

Liu, X., J. Sheng, and R. Curtiss. 2011. "Fatty Acid Production in Genetically Modified Cyanobacteria." *Proceedings of the National Academy of Sciences of the United States of America* 108: 6899–6904. https://doi.org/10.1073/pnas.1103014108.

Lucius, S., and M. Hagemann. 2024. "The Primary Carbon Metabolism in Cyanobacteria and Its Regulation." *Frontiers in Plant Science* 15: 1417680. https://doi.org/10.3389/fpls.2024.1417680.

Lucius, S., M. Theune, S. Arrivault, et al. 2022. "CP12 Fine-Tunes the Calvin-Benson Cycle and Carbohydrate Metabolism in Cyanobacteria." *Frontiers in Plant Science* 13: 1028794. https://doi.org/10.3389/fpls.2022.1028794.

McGenity, T. J., A. T. Crombie, and J. C. Murrell. 2018. "Microbial Cycling of Isoprene, the Most Abundantly Produced Biological Volatile Organic Compound on Earth." *ISME Journal* 12: 931–941. https://doi.org/10.1038/s41396-018-0072-6.

Menin, B., A. Lami, S. Musazzi, A. A. Petrova, S. Santabarbara, and A. P. Casazza. 2019. "A Comparison of Constitutive and Inducible Non-Endogenous Keto-Carotenoids Biosynthesis in *Synechocystis* sp. PCC 6803." *Microorganisms* 7: 501. https://doi.org/10.3390/microorganisms7110501.

Miao, R., M. Jahn, K. Shabestary, G. Peltier, and E. P. Hudson. 2023. "CRISPR Interference Screens Reveal Growth-Robustness Tradeoffs in *Synechocystis* sp. PCC 6803 Across Growth Conditions." *Plant Cell* 35: 3937–3956. https://doi.org/10.1093/plcell/koad208.

Miao, R., H. Xie, and P. Lindblad. 2018. "Enhancement of Photosynthetic Isobutanol Production in Engineered Cells of *Synechocystis* PCC 6803." *Biotechnology for Biofuels* 11: 267. https://doi.org/10.1186/s13068-018-1268-8.

Mustila, H., A. Kugler, and K. Stensjö. 2021. "Isobutene Production in *Synechocystis* sp. PCC 6803 by Introducing α-Ketoisocaproate Dioxygenase From *Rattus norvegicus*." *Metabolic Engineering Communications* 12: e00163. https://doi.org/10.1016/j.mec.2021.e00163.

Nielsen, A. Z., S. B. Mellor, K. Vavitsas, et al. 2016. "Extending the Biosynthetic Repertoires of Cyanobacteria and Chloroplasts." *Plant Journal* 87: 87–102. https://doi.org/10.1111/tpj.13173.

Nilsson, A., K. Shabestary, M. Brandão, and E. P. Hudson. 2020. "Environmental Impacts and Limitations of Third-Generation Biobutanol: Life Cycle Assessment of n-Butanol Produced by Genetically

14677652, 2026, 3, Downloaded from https://onlinelibrary.wiley.com/doi/10.1111/pbi.70395 by Uppsala University, Wiley Online Library on [27/05/2026]. See the Terms and Conditions (https://onlinelibrary.wiley.com/terms-and-conditions) on Wiley Online Library for rules of use; OA articles are governed by the applicable Creative Commons License

Engineered Cyanobacteria." *Journal of Industrial Ecology* 24: 205–216. https://doi.org/10.1111/jiec.12843.

Oliver, J. W. K., I. M. P. Machado, H. Yoneda, and S. Atsumi. 2013. "Cyanobacterial Conversion of Carbon Dioxide to 2,3-Butanediol." *Proceedings of the National Academy of Sciences of the United States of America* 110: 1249–1254. https://doi.org/10.1073/pnas.1213024110.

Pade, N., S. Erdmann, H. Enke, et al. 2016. "Insights Into Isoprene Production Using the Cyanobacterium *Synechocystis* sp. PCC 6803." *Biotechnology for Biofuels* 9: 89. https://doi.org/10.1186/s13068-016-0503-4.

Perez-Gil, J., J. Behrendorff, A. Douw, and C. E. Vickers. 2024. "The Methylerythritol Phosphate Pathway as an Oxidative Stress Sense and Response System." *Nature Communications* 15: 5303. https://doi.org/10.1038/s41467-024-49483-8.

Pollastri, S., I. Baccelli, and F. Loreto. 2021. "Isoprene: An Antioxidant Itself or a Molecule With Multiple Regulatory Functions in Plants?" *Antioxidants (Basel)* 10: 684. https://doi.org/10.3390/antiox10050684.

Pollastri, S., I. Jorba, T. J. Hawkins, et al. 2019. "Leaves of Isoprene-Emitting Tobacco Plants Maintain PSII Stability at High Temperatures." *New Phytologist* 223: 1307–1318. https://doi.org/10.1111/nph.15847.

Porra, R. J., W. A. Thompson, and P. E. Kriedemann. 1989. "Determination of Accurate Extinction Coefficients and Simultaneous Equations for Assaying Chlorophylls *a* and *b* Extracted With Four Different Solvents: Verification of the Concentration of Chlorophyll Standards by Atomic Absorption Spectroscopy." *Biochimica et Biophysica Acta—Bioenergetics* 975: 384–394. https://doi.org/10.1016/S0005-2728(89)80347-0.

Rana, A., L. C. Gomes, J. S. Rodrigues, et al. 2022. "A Combined Photobiological–Photochemical Route to C10 Cycloalkane Jet Fuels From Carbon Dioxide via Isoprene." *Green Chemistry* 24: 9602–9619. https://doi.org/10.1039/D2GC03272D.

Rodrigues, J. S., L. Kovács, M. Lukeš, et al. 2023. "Characterizing Isoprene Production in Cyanobacteria—Insights Into the Effects of Light, Temperature, and Isoprene on *Synechocystis* sp. PCC 6803." *Bioresource Technology* 380: 129068. https://doi.org/10.1016/j.biortech.2023.129068.

Rodrigues, J. S., and P. Lindberg. 2021a. "Engineering Cyanobacteria as Host Organisms for Production of Terpenes and Terpenoids." In *Cyanobacteria Biotechnology*, 267–300. John Wiley & Sons, Ltd. https://doi.org/10.1002/9783527824908.ch9.

Rodrigues, J. S., and P. Lindberg. 2021b. "Metabolic Engineering of *Synechocystis* sp. PCC 6803 for Improved Bisabolene Production." *Metabolic Engineering Communications* 12: e00159. https://doi.org/10.1016/j.mec.2020.e00159.

Rohmer, M., M. Seemann, S. Horbach, S. Bringer-Meyer, and H. Sahm. 1996. "Glyceraldehyde 3-Phosphate and Pyruvate as Precursors of Isoprenic Units in an Alternative Non-Mevalonate Pathway for Terpenoid Biosynthesis." *Journal of the American Chemical Society* 118: 2564–2566. https://doi.org/10.1021/ja9538344.

Ruffing, A. M. 2014. "Improved Free Fatty Acid Production in Cyanobacteria With *Synechococcus* sp. PCC 7002 as Host." *Frontiers in Bioengineering and Biotechnology* 2: 17. https://doi.org/10.3389/fbioe.2014.00017.

Rugbjerg, P., and L. Olsson. 2020. "The Future of Self-Selecting and Stable Fermentations." *Journal of Industrial Microbiology & Biotechnology* 47: 993–1004. https://doi.org/10.1007/s10295-020-02325-0.

Schnitzler, J.-P., I. Zimmer, A. Bachl, M. Arend, J. Fromm, and R. J. Fischbach. 2005. "Biochemical Properties of Isoprene Synthase in Poplar (*Populus* × *canescens*)." *Planta* 222: 777–786. https://doi.org/10.1007/s00425-005-0022-1.

Sengupta, A., P. Pritam, D. Jaiswal, A. Bandyopadhyay, H. B. Pakrasi, and P. P. Wangikar. 2020. "Photosynthetic Co-Production of Succinate and Ethylene in A Fast-Growing Cyanobacterium, *Synechococcus elongatus* PCC 11801." *Metabolites* 10: 250. https://doi.org/10.3390/metabo10060250.

Shabestary, K., and E. P. Hudson. 2016. "Computational Metabolic Engineering Strategies for Growth-Coupled Biofuel Production by *Synechocystis*." *Metabolic Engineering Communications* 3: 216–226. https://doi.org/10.1016/j.meteno.2016.07.003.

Sharkey, T. D., and S. E. Aspland. 2013. High Efficiency Isoprene Synthases Produced by Protein Engineering WO2013016591A1.

Shastri, A. A., and J. A. Morgan. 2005. "Flux Balance Analysis of Photoautotrophic Metabolism." *Biotechnology Progress* 21: 1617–1626. https://doi.org/10.1021/bp050246d.

Shen, C. R., and J. C. Liao. 2012. "Photosynthetic Production of 2-Methyl-1-Butanol From CO_2 in Cyanobacterium *Synechococcus elongatus* PCC7942 and Characterization of the Native Acetohydroxyacid Synthase." *Energy & Environmental Science* 5: 9574–9583. https://doi.org/10.1039/C2EE23148D.

Sun, T., Z. Li, S. Li, L. Chen, and W. Zhang. 2023. "Exploring and Validating Key Factors Limiting Cyanobacteria-Based CO2 Bioconversion: Case Study to Maximize *Myo*-Inositol Biosynthesis." *Chemical Engineering Journal* 452: 139158. https://doi.org/10.1016/j.cej.2022.139158.

Ungerer, J., and H. B. Pakrasi. 2016. "Cpf1 Is A Versatile Tool for CRISPR Genome Editing Across Diverse Species of Cyanobacteria." *Scientific Reports* 6: 39681. https://doi.org/10.1038/srep39681.

Ungerer, J., L. Tao, M. Davis, M. Ghirardi, P.-C. Maness, and J. Yu. 2012. "Sustained Photosynthetic Conversion of CO_2 to Ethylene in Recombinant Cyanobacterium *Synechocystis* 6803." *Energy & Environmental Science* 5: 8998–9006. https://doi.org/10.1039/C2EE22555G.

Vickers, C. E., M. Possell, C. I. Cojocariu, et al. 2009. "Isoprene Synthesis Protects Transgenic Tobacco Plants From Oxidative Stress." *Plant, Cell & Environment* 32: 520–531. https://doi.org/10.1111/j.1365-3040.2009.01946.x.

Volke, D. C., J. Rohwer, R. Fischer, and S. Jennewein. 2019. "Investigation of the Methylerythritol 4-Phosphate Pathway for Microbial Terpenoid Production Through Metabolic Control Analysis." *Microbial Cell Factories* 18: 192. https://doi.org/10.1186/s12934-019-1235-5.

Wedel, N., and J. Soll. 1998. "Evolutionary Conserved Light Regulation of Calvin Cycle Activity by NADPH-Mediated Reversible Phosphoribulokinase/CP12/ Glyceraldehyde-3-Phosphate Dehydrogenase Complex Dissociation." *Proceedings of the National Academy of Sciences* 95: 9699–9704. https://doi.org/10.1073/pnas.95.16.9699.

Whited, G. M., F. J. Feher, D. A. Benko, et al. 2010. "Technology Update: Development of a Gas-Phase Bioprocess for Isoprene-Monomer Production Using Metabolic Pathway Engineering." *Industrial Biotechnology* 6: 152–163. https://doi.org/10.1089/ind.2010.6.152.

Włodarczyk, A., T. T. Selão, B. Norling, and P. J. Nixon. 2020. "Newly Discovered *Synechococcus* sp. PCC 11901 Is a Robust Cyanobacterial Strain for High Biomass Production." *Communications Biology* 3: 1–14. https://doi.org/10.1038/s42003-020-0910-8.

Yang, D. H., J. Webster, Z. Adam, M. Lindahl, and B. Andersson. 1998. "Induction of Acclimative Proteolysis of the Light-Harvesting Chlorophyll a/b Protein of Photosystem II in Response to Elevated Light Intensities." *Plant Physiology* 118: 827–834. https://doi.org/10.1104/pp.118.3.827.

Yao, L., F. Qi, X. Tan, and X. Lu. 2014. "Improved Production of Fatty Alcohols in Cyanobacteria by Metabolic Engineering." *Biotechnology for Biofuels* 7: 94. https://doi.org/10.1186/1754-6834-7-94.

Ye, L., X. Lv, and H. Yu. 2016. "Engineering Microbes for Isoprene Production." *Metabolic Engineering* 38: 125–138. https://doi.org/10.1016/j.ymben.2016.07.005.

14677652, 2026, 3, Downloaded from https://onlinelibrary.wiley.com/doi/10.1111/pbi.70395 by Uppsala University, Wiley Online Library on [27/05/2026]. See the Terms and Conditions (https://onlinelibrary.wiley.com/terms-and-conditions) on Wiley Online Library for rules of use; OA articles are governed by the applicable Creative Commons License

Yunus, I. S., and P. R. Jones. 2018. "Photosynthesis-Dependent Biosynthesis of Medium Chain-Length Fatty Acids and Alcohols." *Metabolic Engineering* 49: 59–68. https://doi.org/10.1016/j.ymben.2018.07.015.

Yunus, I. S., A. Palma, D. L. Trudeau, D. S. Tawfik, and P. R. Jones. 2020. "Methanol-Free Biosynthesis of Fatty Acid Methyl Ester (FAME) in *Synechocystis* sp. PCC 6803." *Metabolic Engineering* 57: 217–227. https://doi.org/10.1016/j.ymben.2019.12.001.

Zavřel, T., P. Očenášová, and J. Červený. 2017. "Phenotypic Characterization of *Synechocystis* sp. PCC 6803 Substrains Reveals Differences in Sensitivity to Abiotic Stress." *PLoS One* 12: e0189130. https://doi.org/10.1371/journal.pone.0189130.

Zhou, J., H. Zhang, H. Meng, Y. Zhang, and Y. Li. 2014. "Production of Optically Pure d-Lactate From CO2 by Blocking the PHB and Acetate Pathways and Expressing d-Lactate Dehydrogenase in Cyanobacterium *Synechocystis* sp. PCC 6803." *Process Biochemistry* 49: 2071–2077. https://doi.org/10.1016/j.procbio.2014.09.007.

Zhou, J., H. Zhang, Y. Zhang, Y. Li, and Y. Ma. 2012. "Designing and Creating a Modularized Synthetic Pathway in Cyanobacterium *Synechocystis* Enables Production of Acetone From Carbon Dioxide." *Metabolic Engineering* 14: 394–400. https://doi.org/10.1016/j.ymben.2012.03.005.

Supporting Information

Additional supporting information can be found online in the Supporting Information section. **Figure S1:** Semi-quantitative Western blot analysis from the membrane shown in Figures 2C,D and 3A. (A) Flag-IspS signal intensity normalised to AtpB from the Western blot membrane shown in Figure 2C. (B) Flag-IspS signal intensity normalised to AtpB from the Western blot membrane shown in Figure 2D. (C) Flag-IspS signal intensity normalised to AtpB from the Western blot membrane shown in Figure 3A. (D) Relative Flag-IspS signal intensity plotted from a–c plotted against relative isoprene production displayed in the corresponding Figures 2C,D and 3A. Relative Flag-IspS signal intensity, as well as isoprene production was normalised to the values of KJ05. **Figure S2:** Genotyping of engineered strains. (A) CRISPR-Cas12 deletion of the Km resistance gene from 1-IspS. Primers binding to EgIspS (fw) and downstream neutral site 1 (rv), expected sizes: with KmR 2.7 kb; without KmR 1.7 kb. (B) *phaAB* locus with primers binding upstream and downstream of the homology arms used for homologous recombination. Expected sizes: WT 3.1 kb; CmR 2.1 kb, EgIspS 4.0 kb, IspHG 5.0 kb. (C) *cp12* locus with primers binding upstream and downstream of the homology arms used for homologous recombination. Expected sizes: WT 1.4 kb; CmR 2.2 kb; EgIspS 4.1 kb. (D) *ddh* locus with primers binding upstream and downstream of the homology arms used for homologous recombination (upper panel). Expected sizes: WT 3.2 kb, EmR 3.3 kb, EgIspS 5.3 kb. (E) *Ddh* locus with primers binding to the WT *ddh* gene (fw) and downstream genomic region (rv) to confirm absence of WT sequence in engineered strains. Expected sizes: WT 2.0 kb, no band upon deletion of WT sequence. **Figure S3:** Dissolved O_2 levels and isoprene productivity in response to light intensity increase from 250 to 500 μmol photons $m^{-2} s^{-1}$ during stirred tank photobioreactor cultivation. **Figure S4:** Specific CO_2 uptake rates during the bioreactor experiment shown in Figure 4. **Table S1:** *Synechocystis* PCC6803 strains used and generated in this study. **Table S2:** Primers used in this study. **Table S3:** Linear growth rates of selected strains cultivated with ambient CO_2 (LC) and supplemented with 50 mM sodium bicarbonate every three days (HC) during batch cultivation [day^{-1}]. **Table S4:** *Synechocystis* PCC6803 genes and loci used as insertion sites or for overexpression. **Table S5:** Plasmids generated in this study.

14677652, 2026, 3, Downloaded from https://onlinelibrary.wiley.com/doi/10.1111/pbi.70395 by Uppsala University, Wiley Online Library on [27/05/2026]. See the Terms and Conditions (https://onlinelibrary.wiley.com/terms-and-conditions) on Wiley Online Library for rules of use; OA articles are governed by the applicable Creative Commons License